

# **Hand-Held Radiometry**

*A Set of Notes Developed for Use at the  
Workshop on Hand-Held Radiometry  
Phoenix, Ariz., February 25-26, 1980*

U.S. Department of Agriculture  
Science and Education Administration  
Agricultural Reviews and Manuals • ARM-W-19/October 1980



# **Hand-Held Radiometry**

*A Set of Notes Developed for Use at the  
Workshop on Hand-Held Radiometry  
Phoenix, Ariz., February 25-26, 1980*

**by Ray D. Jackson, Paul J. Pinter, Jr.**

**Robert J. Reginato, and Sherwood B. Idso**

U.S. Department of Agriculture  
Science and Education Administration  
Agricultural Reviews and Manuals • ARM-W-19/October 1980

This portable document file version (PDF, Adobe Acrobat8) has been prepared by scanning an original hardcopy of this publication and converting the text using optical character recognition software. Every attempt was made to catch errors in the translation process, but it is likely that many still remain. Readers should also be aware that many advances have been made in the field of remote sensing, new technologies are now available, and some of the concepts that we advance in this 1980 publication are now out of date.

Please notify Paul Pinter by email ([ppinter@uswcl.ars.ag.gov](mailto:ppinter@uswcl.ars.ag.gov)) with a written description of any serious errors you discover and we will try to fix them. The original paper document is still available upon request from the Librarian, USDA, ARS, U.S. Water Conservation Laboratory, 4331 East Broadway Road, Phoenix, Arizona 85040. Additional resources not originally in the Handbook can be found on the USWCL Website which is located at <http://www.uswcl.ars.ag.gov>.

The original document was scanned and converted by Ms. Suzette Maneely, Biological Science Technician at the U.S. Water Conservation Laboratory. (June 2001)

International Standard Serial Number (ISSN) 0193-3760

Science and Education Administration, Agricultural Reviews and Manuals, Western Series, No. 19, October 1980

---

Published by Agricultural Research (Western Region), Science and Education Administration, U.S. Department of Agriculture, Oakland, Calif. 94612

## ABSTRACT

Hand-held radiometers are small instruments that measure radiation that has been reflected or emitted from a target. Most have bandpass regions similar to those of scanners aboard satellites now in orbit or soon to be launched. Hand-held radiometers are particularly useful for obtaining frequent spectral and thermal data over numerous small plots having different treatments such as irrigations or fertilization. Such experiments allow the development of relationships between remotely sensed data and agronomic variables, as well as relationships needed for improved interpretation of satellite data and their applications to agriculture.

A set of notes was developed to aid the beginner in hand-held radiometry. The electromagnetic spectrum is reviewed, and pertinent terms are defined. View areas of multiband radiometers are developed to show the areas of coincidence of adjacent bands. The amounts of plant cover seen by radiometers having different fields of view are described. Vegetation indices are derived and discussed. Response functions of several radiometers are shown and applied to spectrometer data taken over 12 wheat plots, to provide a comparison of instruments and bands within and among instruments. The calculation of solar time is reviewed and applied to the calculation of the local time of LANDSAT satellite overpasses for any particular location in the northern hemisphere. The use and misuse of hand-held infrared thermometers are discussed, and a procedure for photographic determination of plant cover is described.

Some suggestions are offered concerning procedures to be followed when collecting hand-held spectral and thermal data. A list of references pertinent to hand-held radiometry is included.

**KEYWORDS:** Hand-held radiometers, remote sensing, reflectance spectra, thermal infrared, vegetation indices.

#### ACKNOWLEDGMENTS

We wish to acknowledge the contributions of Craig L. Wiegand, Science and Education Administration-Agricultural Research (SEA-AR), Weslaco, Tex., and Armand Bauer, SEA-AR, Mandan, N. Dak.

We also wish to thank J. K. Aase, SEA-AR, Sidney, Mont., and C. J. Tucker, J. C. Price, and E. Chappelle, NASA/Goddard Space Flight Center, Greenbelt, Md., for the data they furnished.

Trade names and the names of commercial companies are used in this publication solely to provide specific information. Mention of a trade name or manufacturer does not constitute a guarantee or warranty of the product by the U.S. Department of Agriculture nor an endorsement by the Department over other products not mentioned.

## CONTENTS

	Page
Introduction.....	1
The electromagnetic spectrum.....	3
Irradiance, radiance, reflectance, and Lambertian surfaces.....	6
View areas of multiband radiometers.....	8
Area of a sector and a segment of a circle.....	8
Two-band radiometers.....	9
Three-band radiometers.....	9
Four-band radiometers.....	10
Ratios of coincident areas to target areas.....	11
Radiometric plant cover.....	14
Case 1, row spacing = 0.3 m, row width = 0.15 m, FOV = 15°.....	15
Case 2, row spacing = 0.3 m, row width = 0.15 m, FOV = 24°.....	16
Case 3, row spacing = 1 m, row width = 0.5 m, FOV = 15°.....	17
Vegetation indices.....	21
Ratios.....	22
Normalized difference.....	24
Transformed normalized difference.....	24
Numerical example.....	25
Perpendicular vegetation index.....	27
The soil line.....	29
Some calculated results.....	31
Radiometer response functions.....	34
Relative response functions for four radiometers.....	35
Field spectrometer data.....	36
Comparison of bands among instruments.....	38
Comparison of vegetation indices among instruments.....	41
The water absorption band.....	42
Calculation of approximate local standard time for LANDSAT overpasses.....	43
Time.....	45
LANDSAT overpass times.....	48
Infrared thermometers.....	51
Field use.....	52
Calibrations.....	52
Precautions.....	53
a) Temperature equilibrium and warm-up periods.....	53
b) Operation in a noisy environment.....	53
c) Operation in a dusty environment.....	53
d) Miscellaneous precautions and procedures.....	53
Photographic determination of canopy cover.....	54
Standardization of measurements and recording of environmental conditions.....	55
Procedures in support of hand-held radiometer observations.....	57
Hand-held radiometer measurements.....	57
Plant observations.....	59
Weather data.....	60
Sampling.....	60
Ground photography.....	61
Terminology.....	61
Selected references.....	61

---

## HAND-HELD RADIOMETRY

By Ray D. Jackson, Paul J. Pinter, Jr.,  
Robert J. Reginato, and Sherwood B. Idso<sup>1</sup>

### INTRODUCTION

Light from the sun, reflected from soils and plants, can tell us how much plant material is present in the field, the vigor of the plants, whether plant diseases or insects have caused damage, and other aspects important to the production of food and fiber. Since 1972, the National Aeronautics and Space Administration (NASA) has launched three satellites (called LANDSATs) that carry multispectral scanners (MSS), instruments that measure reflected light in particular wavelength bands. Future satellites of this general type will also have a band that measures emitted thermal radiation, from which surface temperatures can be inferred. The exploitation of satellite information for agricultural research and for management decisions is hampered by the frequency of coverage (once every 18 days, if cloud free) and the time required to process the data. In addition, research data concerning the fundamental relationships between reflected and emitted radiation and various agronomic factors found in field situations is minimal. Recent advances in electronic technology now allow the construction of small instruments that mimic the satellite scanners but can be carried and operated by one person. We call these instruments hand-held radiometers.

For research purposes, and to aid in the interpretation of satellite data, relationships must be developed between remotely sensed spectral data and agronomic variables such as leaf area index, biomass, and amount of ground cover. Such relationships can best be developed by obtaining spectral data over numerous small plots where crops are carefully monitored and researchers can exercise some manipulation of cultural variables such as soil water and row orientation. Hand-held radiometers are ideally suited for these types of experiments because of their portability. Many measurements can be made rapidly in experimental fields inaccessible to vehicles and too small to be included in the resolution element of aircraft- or satellite-based sensors. Additional detail on the usefulness of hand-held radiometry was given by Tucker (1978b).<sup>2</sup>

<sup>1</sup> Physicist, entomologist, soil scientist, and physicist, respectively, Science and Education Administration, Agricultural Research (SEA/AR), U.S. Water Conservation Laboratory, 4331 East Broadway Road, Phoenix, Ariz. 85040.

<sup>2</sup> The year in italic, when it follows the author's name, refers to Selected References, p. 61.

An important aspect of remote sensing research is the problem of comparing data taken with various instruments having different characteristics. Some questions that should be addressed within this context are: How do you compare data obtained from radiometers that measure radiation in different wavelength regions? How do you relate data taken with a wide field of view (15° for most hand-held instruments) to data obtained with different fields of view, or to an aircraft- or satellite- based scanner where the instantaneous field of view is very small? What does an instrument see in terms of plants and soil back ground? What are "vegetation indices," and how are they used? The overriding question is: How can we best take spectral data that are understandable and transferable to other situations?

In 1979, the SEA/AR Wheat Yield Modeling Group contracted with NASA to construct approximately 12 hand-held radiometers for delivery in 1980. These radiometers, designed by Tucker et al. (1980) at the Goddard Space Flight Center (GSFC), contain three bands that are similar to three bands of the Thematic Mapper, the radiometer that is to be carried on LANDSAT-D (scheduled for launch as LANDSAT-4 in 1981) (Tucker 1978a). This instrument, designated as the Mark II 3-band, was developed after Tucker had gained a considerable amount of experimental experience with a two-band instrument described by Pearson et al. (1976) (herein called the PMT 2-band). Another radiometer adaptable to hand-held use has been available commercially for several years. This is the Exotech model 100A "LANDSAT Ground Truth" radiometer, whose bands, as the name implies, correspond to bands 4 through 7 on the MSS carried by the currently orbiting LANDSATs. All of these instruments measure portions of the electromagnetic spectrum that are in the visible and the near infrared (IR) regions.

Our introduction to hand-held spectral radiometers occurred after a meeting in January 1977 with Barrett Robinson and Marvin Bauer of the Laboratory for Applications of Remote Sensing (LARS), Purdue University. They loaned us equipment, and Barrett Robinson spent a day instructing us in the use of the Exotech model 100A. We are starting our fourth year of measurements with the Exotech, but due to weather conditions and a few other reasons, we have little field experience with the Mark II 3-band.

Many of the same researchers who will be using these instruments to measure reflected radiation have also ordered a newly developed hand-held IR "thermometer" that measures emitted thermal radiation in the 8 to 14  $\mu\text{m}$  (or 10.5 to 12.5  $\mu\text{m}$ ) wavelength regions, which can be related to surface temperatures. This instrument, produced by the Telatemp Corporation, weighs about 1.1 kg and has a pistol grip, which allows it to be held like a handgun. We have used the Telatemp for 2 years; and for 4 years preceding that we used a Barnes PRT-5 IR thermometer.

During these years, we have learned a bit about the use of hand-held radiometers--much of it by trial and error--and as in most endeavors, hindsight has been an excellent teacher. Thus, with the impending deliveries of hand-held radiometers to our colleagues, we thought that a workshop, in which we discussed much of what we know about the use and misuse of hand-held radiometers, would be beneficial.

In preparing for the workshop, a set of notes developed. We share these notes with a word of caution: We do not have all the answers, some things may

not be completely precise, and a few errors are bound to be disguised as facts. Nevertheless, we hope that they will serve a useful purpose. We have cited some literature and added other pertinent references, but no comprehensive review was attempted. We thank Craig Wiegand, SEA/AR, Weslaco, Tex., and C. Jim Tucker, NASA, Greenbelt, Md., who were very helpful in providing information and assistance to us during the development of these notes. Thanks also go to Armand Bauer, SEA/AR, Mandan, N. Dak., who gave us permission to reproduce his letter setting out suggestions for standardization of experiments, and to J. K. Aase, SEA/AR, Sidney, Mont., and J. C. Price and E. Chappelle, NASA/ GSFC, who provided us with data.

### THE ELECTROMAGNETIC SPECTRUM

A brief review of the electromagnetic spectrum may be useful for those of us whose sophomore physics is a part of the far distant past. For a detailed discussion, see Suits (1975).

Electromagnetic radiation is a form of energy derived from oscillating magnetic and electrostatic fields. It is capable of being transmitted through space with a velocity  $c = 3 \times 10^8$  m/s. The frequency ( $\nu$ ) of electromagnetic radiation is

$$c = \lambda \nu \tag{1}$$

related to its wavelength ( $\lambda$ ) by

Equation 1 shows that the frequency is inversely proportional to the wavelength. An aid to the visualization of this relationship is given in figure 1. It is emphasized that the figure is merely a representation in

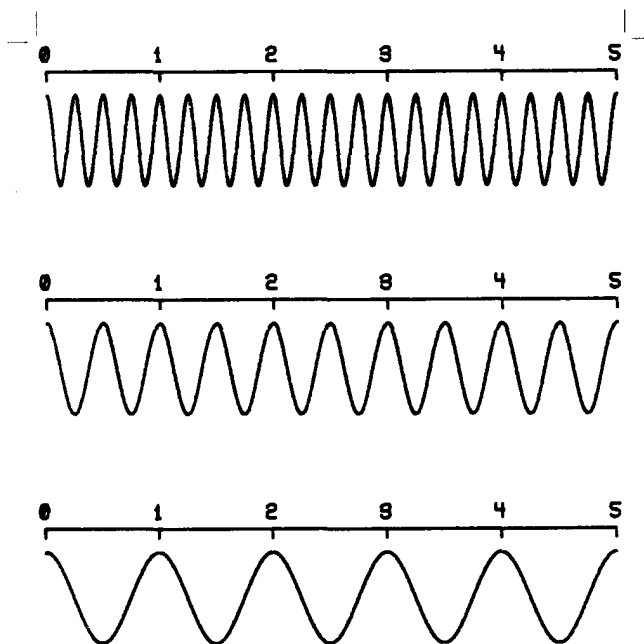


Figure 1.--Graphs of the cosine. These curves facilitate the visualization of the relationship between wavelength and frequency.

that the proportionality constant was taken as 1 (for diagrammatic purposes) instead of the speed of light ( $3 \times 10^8$  m/s) and that cosine curves are not necessarily the true representation of radiation waves. With this in mind, figure 1, top, shows a cosine with a frequency of 4 and a wavelength of  $1/4$ . The center curve is a cosine with a frequency of 2 and a wavelength of  $1/2$ . At the bottom, the frequency is 1 and the wavelength is 1. Thus, we see that as the wavelength increases the frequency decreases.

The electromagnetic spectrum is diagrammed in figure 2 in terms of both wavelength and frequency. Note that wavelengths change from the short, but high energy, gamma rays at  $3 \times 10^{-2}$  Angstroms ( $\text{\AA}$ ) to the long sound waves at 300 km, a factor of  $10^{17}$ , and that the visible range is only a small part of the entire spectrum.

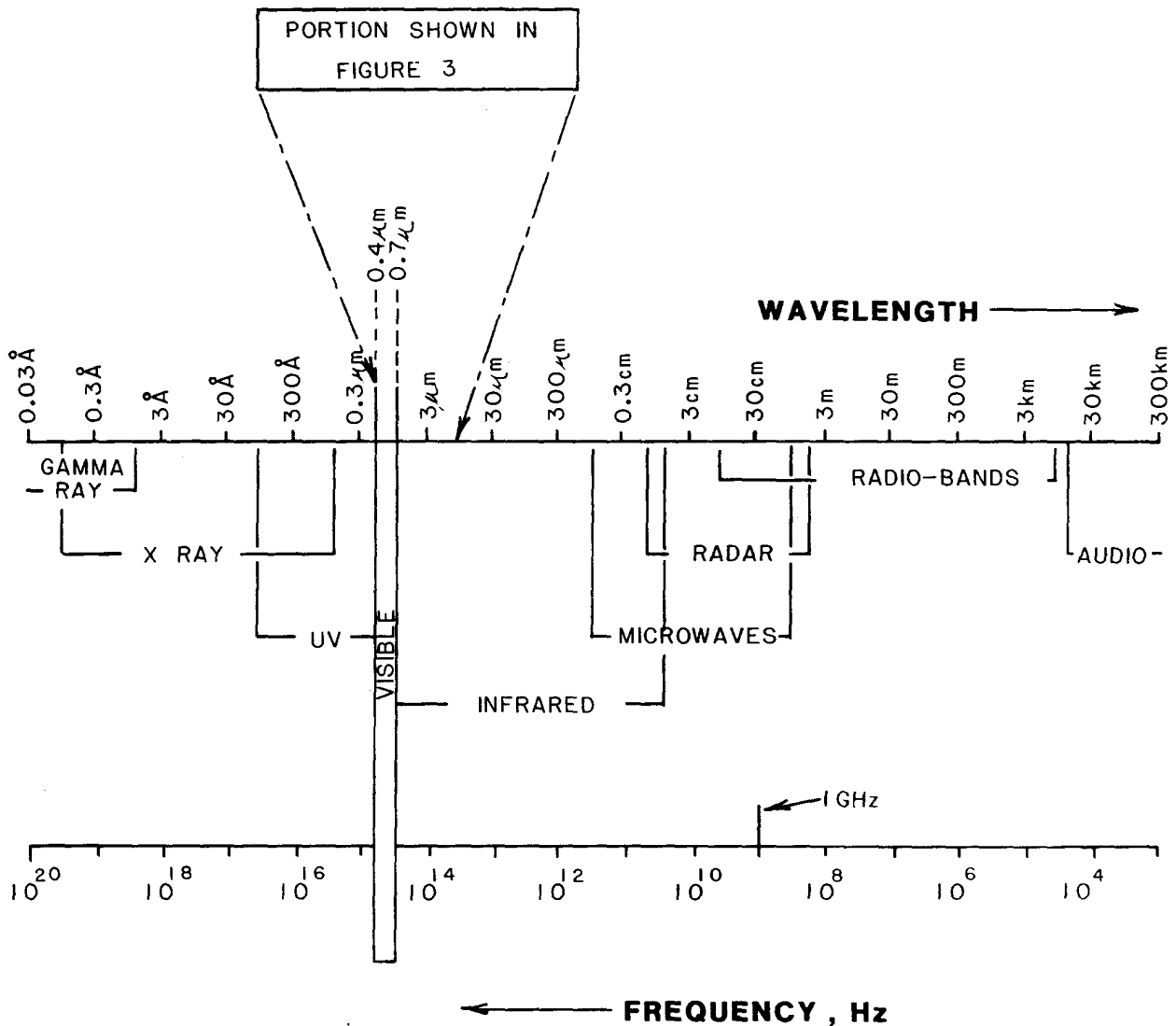


Figure 2.--The electromagnetic spectrum.

Although some remote sensors utilize gamma rays and the ultraviolet, most use the visible, IR, and microwave. Our concern here is with the visible and IR. However, important progress is being made in using active (radar) and passive microwaves to remotely sense agricultural scenes.

In figure 3, the visible and IR portions of the spectrum are expanded. Numbers on the log scale indicate wavelength in micrometers. Near, intermediate, and far IR regions are shown. The portion of the IR region most useful for temperature measurements is between 8 and 14  $\mu\text{m}$ . Portable IR thermometers are available with either an 8- to 14- $\mu\text{m}$  lens or a narrower 10.5- to 12.5- $\mu\text{m}$  lens. The narrower window is most often used on satellite and aircraft based sensors because less atmospheric absorption occurs in the narrower region.

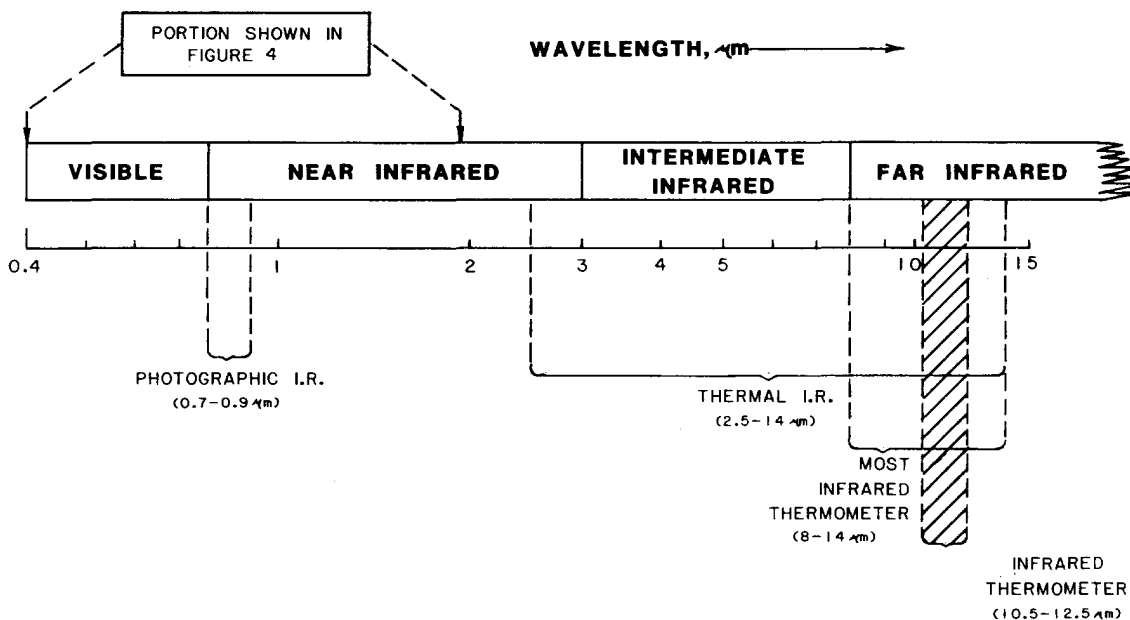


Figure 3.-- A portion of the electromagnetic spectrum relating photographic infrared, thermal infrared, and infrared thermometer ranges to the visible and infrared regions.

The thermal IR region is frequently confused with the photographic IR. Photographic IR is the transition region from the visible to the near IR. Color IR film is sensitive to radiation up to about 0.9  $\mu\text{m}$ , much shorter than the wavelengths of the thermal IR.

The visible and near IR regions are expanded in figure 4. The approximate wavelength intervals for LANDSAT and the Exotech (shown as MSS bands), the PMT 2-band, and the Mark II 3-band are shown. The red bands for the PMT and Mark II instruments are nearly the same and both fall entirely within the MSS5 band of the Exotech and LANDSAT. In the IR, the PMT and the Mark II have their lower wavelength limit within the MSS6 band and their upper limits within the MSS7 band. The Mark II has a third band in 1.55- to 1.75- $\mu\text{m}$  region. This is called the water absorption band, as it is reported to be sensitive to water in vegetation.

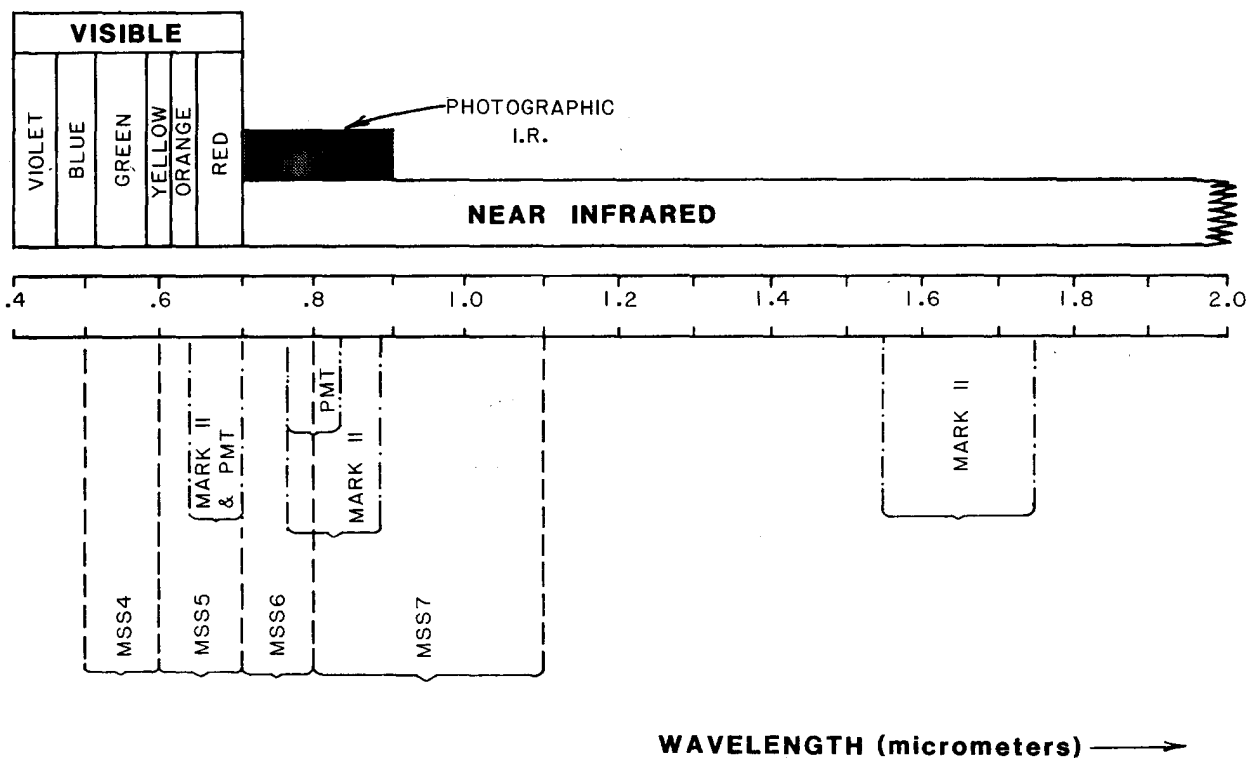


Figure 4.--A portion of the electromagnetic spectrum which includes components of the visible range and most of the near infrared. Approximate wavelength intervals for LANDSAT and the Exotech (MSS) and for the PMT and the Mark II are shown.

## IRRADIANCE, RADIANCE, REFLECTANCE, AND LAMBERTIAN SURFACES

Two terms that are used extensively in remote sensing research are radiance and reflectance. They are easily confused with one another. We will attempt to give a simple explanation here. For detailed discussions, see Silva (1978) and Suits (1975).

On a sunny day, a target (e.g., a wheat field) receives both direct and diffuse solar radiation. This incoming radiation is called irradiance, symbol  $E$ , units of watts per meter<sup>2</sup> ( $Wm^{-2}$ ). When the radiation strikes the target, some is reflected, some is absorbed, and some is transmitted. The ability of substances (e.g., soils and plants) to reflect, absorb, and transmit this radiation varies considerably, thus presenting us with a method of extracting information about the substances. The radiation that is reflected from the target is called radiance, symbol  $L$ , units of  $Wm^{-2}$ . A hand-held radiometer receives radiation reflected from a target in a direction within the field of view of the instrument. The sensors within the instrument react to the radiance and produce a voltage that can be measured, and by calibration, related to the radiance. We can write

$$L = CV \quad (2)$$

where C is a calibration factor and V is the voltage response of the instrument to the radiance L.

We stated earlier that the radiance was radiation that was reflected from a target, implying that the amount reflected is a property of the substance constituting the target. This property is called the reflectance, symbol R, unitless, with values always less than one. Thus

$$L=ER \tag{3}$$

From equation 3, we see that, with R constant, L is directly proportional to the irradiance. This relationship limits the direct use of radiance measurements since the irradiance must also be specified. An obvious solution to this problem is to calculate reflectances; however, this requires a measurement of E. A good approximation of E can be obtained by measuring the radiance from a target of known reflectance.

Standard reflectance plates can be made by carefully applying a special BaSO<sub>4</sub> paint to a flat metal plate after proper pretreatment of the metal; also, BaSO<sub>4</sub> powder can be pressed into a flat sheet (for a discussion of reflectance standards, see Robinson and Biehl, 1979). Standard plates of this type are highly reflective, on the order of 90 to 95 percent. When viewed at angles from 0 (nadir) to about 45°, or illuminated from angles less than 45° from vertical, they are usually assumed to be Lambertian surfaces, although there are some deviations. A Lambertian surface, or a "perfectly diffuse" surface, is a surface that reflects equally in all directions. The radiance of a uniformly illuminated Lambertian surface of infinite extent is constant for any viewing angle. Precise definitions and explanations of Lambertian surfaces, reflectance factors, and other terms is beyond the scope of these notes. Silva (1978) presented a thorough discussion of optical terms useful in remote sensing. We recommend reading Silva (1978) and other articles to obtain complete definitions.

A standard BaSO<sub>4</sub> plate, calibrated with a known surface of radiation, will have a constant reflectance R<sub>p</sub>. If we have a plate near the target of interest, we can measure the radiance from the plate to get

$$L_p = ER_p \tag{4}$$

and, in a short interval of time such that E does not change appreciably, measure the unknown target to get

$$L_t = ER_t \tag{5}$$

If we combine equation 4 and 5, we get

$$R_t = R_p L_t / L_p \tag{6}$$

which is the bidirectional reflectance factor of the target (e.g., wheat field). If the target (and the plate) approximate Lambertian surfaces, the reflectance factor R<sub>t</sub> is independent of irradiance and viewing angles; however, cropped fields and soil surfaces are usually not Lambertian. The radiances from these surfaces are dependent upon the angle of illumination and the

viewing angle. The term "bidirectional reflectance factor" is used to indicate the angular dependence of the measurements. In the following sections, we have used the term "reflectance" in a general sense. Where specific measurements with a hand-held radiometer are discussed, the term "bidirectional reflectance factor" may be more appropriate (Robinson and Biehl, 1979).

## VIEW AREAS OF MULTIBAND RADIOMETERS

Multiband radiometers that are small enough to be hand-held usually consist of two or more optical tubes, each containing a lens and detector assembly for a particular bandpass. The tubes are mounted parallel with each other so as to view approximately the same target. Although the tubes may be just a few centimeters apart, the degree of noncoincidence is sufficient to cause different bands to view somewhat different scenes. Thus, over nonhomogeneous targets, such as crops planted in rows, one band may view predominately soil while the second may view mostly plants. The severity of this problem decreases as the height that the radiometer is held above the target increases and the distance between the tubes decreases. For hand-held radiometry, the height that a radiometer can be held above a crop is not sufficient to completely eliminate the problem. It is instructive to examine the geometry of this situation to gain a perspective of its significance.

Area of a sector and a segment of a circle: The areas of coincidence for two or more overlapping circles can be calculated by using formulas for the areas of sectors and segments of a circle (Larsen, 1958). Figure 5 shows a sector of a circle with center at A and radius r. The area of the segment ( $A_s$ ), the portion bounded by the line connecting points B and D and the arc of the circle, is the area of the sector ( $\alpha r^2/2$ ) minus the area of the two triangles of identical area, ABC and ACD. That is,

$$A_s = (r^2/2) (\alpha - \sin \alpha) \quad (7)$$

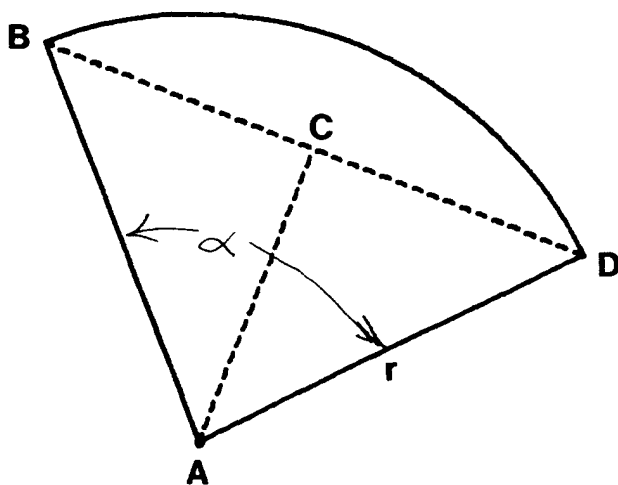


Figure 5.--Sector of a circle. The segment of the sector is the area bounded by the arc of the circle and the line BD.

where  $\alpha = 2 \cos^{-1}(x/r)$ , and  $x$  is the length of the line AC. (8)

Equations 7 and 8 form the basis for calculating coincident target areas for two-, three-, and four-band radiometers.

Two-band radiometers: The coincident area for a two-band radiometer is twice the area of the segment of a circle given by equation 7, i.e.,

$$A_c = r^2 (\alpha - \sin \alpha) \quad (9)$$

here  $x$  to be used in equation 8 is one-half of the distance between centers of the two tubes. Figure 6 shows the target areas and coincident area for a two-band radiometer.

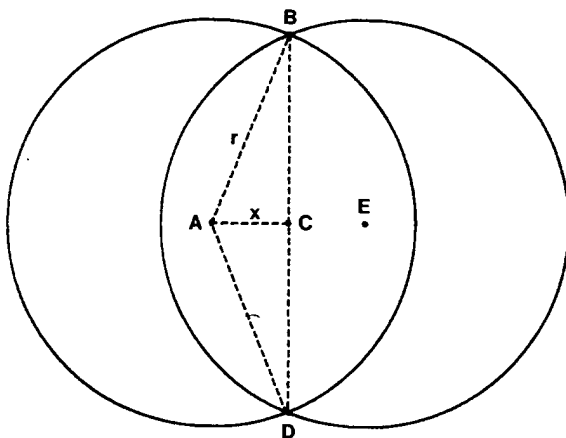


Figure 6.--Coincident area of two overlapping circles of identical radius whose centers are at points A and E.

Three-band radiometers: For a three-band radiometer, the coincident area for any two bands is the same as for a two-band instrument. The coincidence area for all three bands requires a bit more calculation. The geometry is shown in figure 7. We begin at the center of one of the three circles (A) and draw lines to the intersections of two adjoining circles (lines AB and AE). To get one-third of the coincident area, calculate the area of this segment and add the areas of the two triangles BCE and CDE.

The centers of the three tubes form an equilateral triangle. The distance AF =  $x$  is one-half of the distance between the centers of two tubes. The angle subtended by the lines AF and AC is  $\pi/6$ , because it is one-half of one of the  $\pi/3$  angles forming an equilateral triangle. The angle subtending the arc BE is

$$\alpha = 2[\cos^{-1}(x/r) - \pi/6] \quad (10)$$

Using  $\alpha$  in equation 7, yields the area of the segment. The distance BD is  $r \sin(\alpha/2)$ , and the distance CD is  $r \cos(\alpha/2) - x/\cos(\pi/6)$ . The coincident area is

$$A_c = 3\{(r^2/2) (\alpha - \sin \alpha) + r \sin(\alpha/2)[r \cos(\alpha/2) - x/\cos(\pi/6)]\} \quad (11)$$

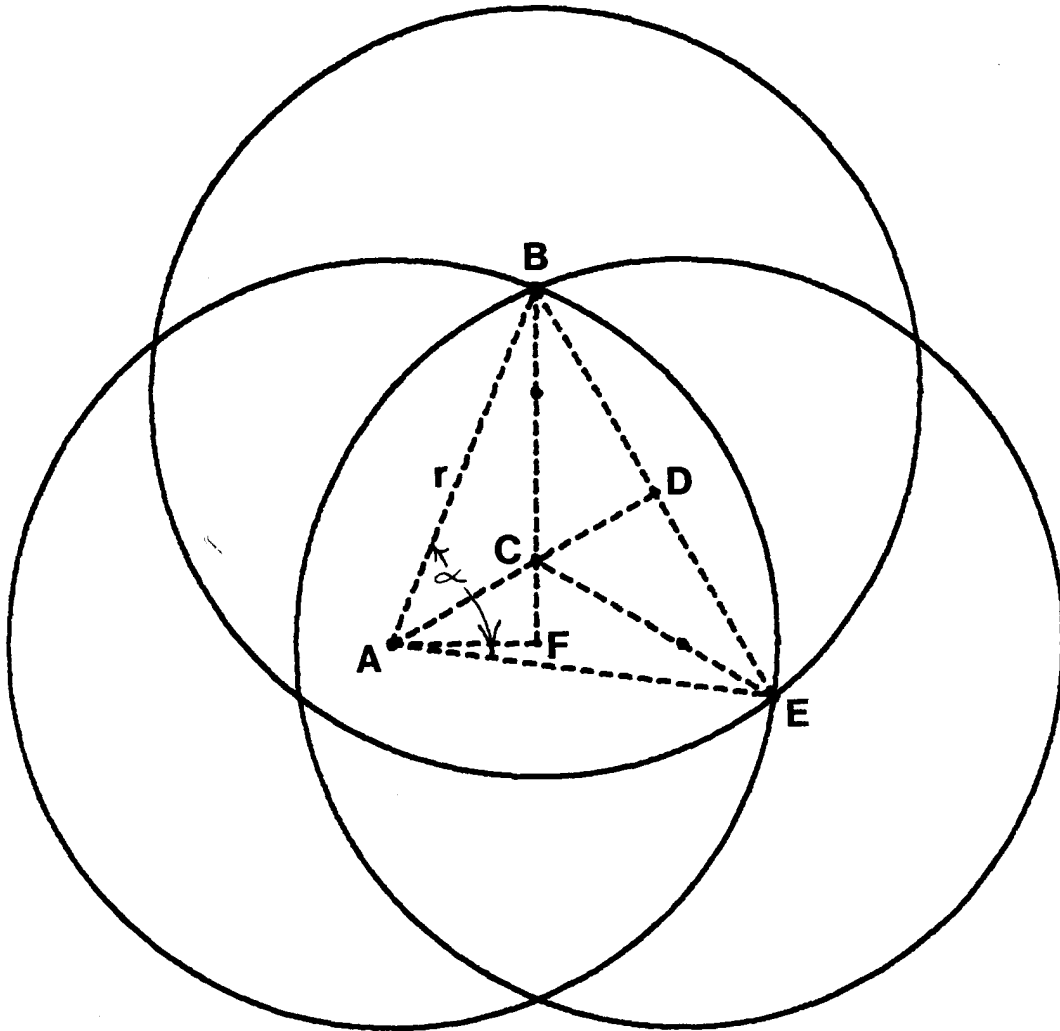


Figure 7.--Coincident area of three overlapping circles whose centers form an equilateral triangle. The distance  $x$  is the length of the line  $AF$  and is one-half of the distance between the centers of two circles.

Four-band radiometers: Calculation of the coincident area for two adjoining tubes of a four-band radiometer is the same as for a two-band instrument. The distance  $x$  is, again, one-half of the distance between the centers of two adjoining tubes. If the four tubes form a rectangle, the coincident area for diagonal tubes can be calculated using equations 8 and 9 with  $x$  being one-half the distance between diagonal tubes, which is the square root of two times the distance between adjoining tubes.

The coincident area for the four tubes can be obtained by calculating the area of a segment, adding the area of two identical triangles, and multiplying by 4. Figure 8 shows the coincident area for four overlapping target areas for a four-band radiometer. The points  $A$ ,  $B$ ,  $E$ , and  $H$  represent centers of the four tubes with a common center at  $C$ . The sector of interest is  $ADG$ . The angle subtending the lines  $AC$  and  $AJ$  is  $\pi/4$ . The angle subtending the arc  $DG$  is

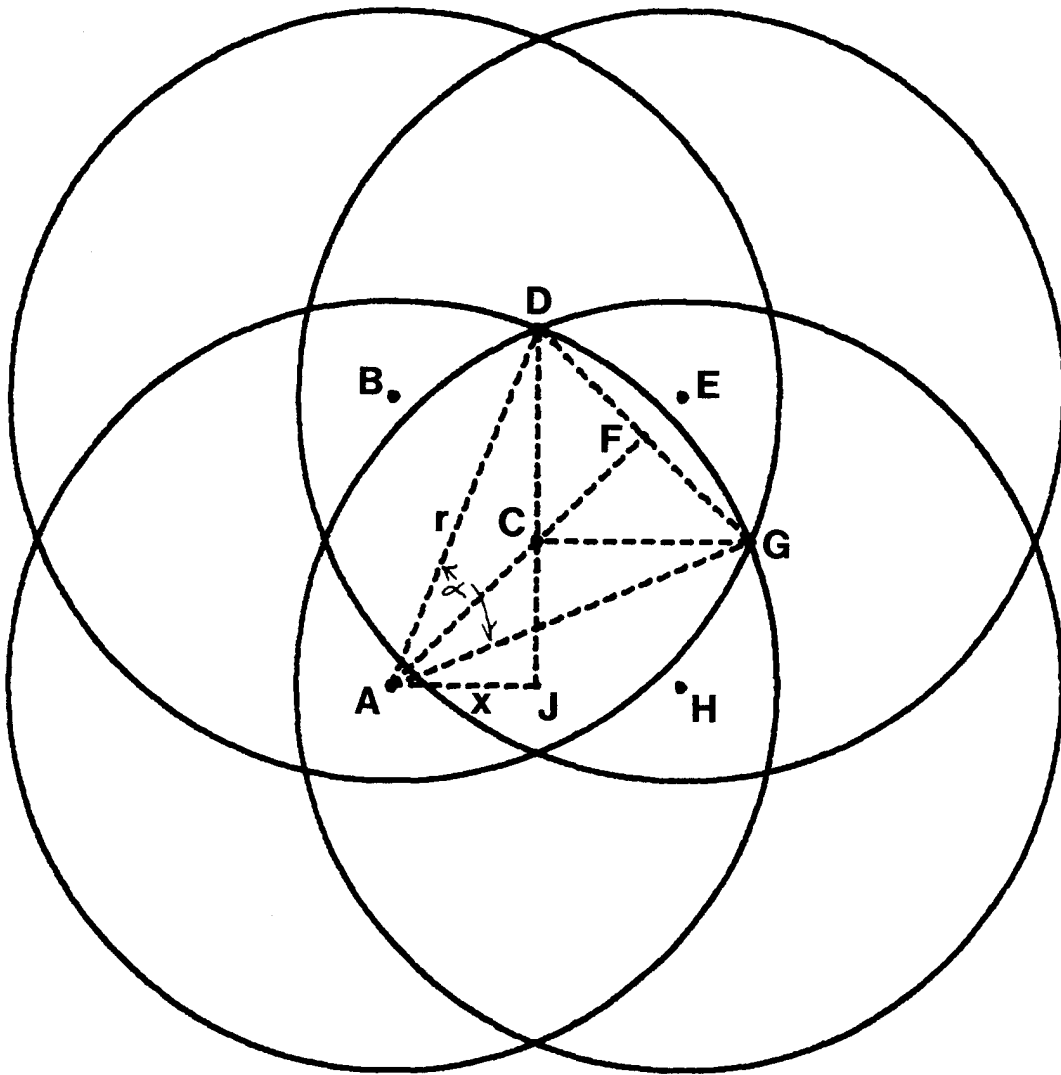


Figure 8.--Coincident area for four overlapping circles whose centers form a square. The distance  $x$  is the length of the line  $AJ$  and is one-half of the distance between centers of adjacent circles.

$$\alpha = 2[\cos^{-1}(x/r) - \pi/4] \quad (12)$$

The distance  $DF$  is  $r \sin(\alpha/2)$  and the distance  $CF$  is  $r \cos(\alpha/2) - 2^{1/2} x$ . The coincident area is

$$A_c = 4\{(r^2/2)(\alpha - \sin \alpha) + r \sin(\alpha/2)[r \cos(\alpha/2) - 2^{1/2}x]\} \quad (13)$$

Ratios of coincident areas to target areas: The ratio of a coincident area to the total target area for a tube can be calculated as a function of height above a target. The closer this ratio approaches 1, the less error will be encountered in the spectral data. For this calculation, we need to specify a field of view (FOV) and the distances between centers of the optical tubes for particular instruments. For this discussion, we will use the Mark II 3-band

radiometer and the Exotech 4-band radiometer. Both instruments have a 15° FOV capability. The distance between tubes for the three-band instrument is 3.8 cm, and 6.35 for the four-band instrument. The relation between the radius of the target area and the height of the radiometer (h) is

$$r = h \tan(\text{FOV}/2) \quad (14)$$

For a 15° FOV,  $r = 0.132 h$ . The diameter of a target circle is 26.4 cm when the radiometer is held at 1 m, and 52.7 cm when held at 2 m. In other words, the diameter is roughly one-fourth of the height that the radiometer is held. This is a useful approximation when estimating target areas over row crops.

Figure 9A shows the ratio of the coincidence area to the target area as a function of the radiometer height above the target for the Mark II 3-band and the Exotech 4-band instruments. At 2 m in height, any two bands of the three-band instrument will view about 91 percent of the same area. At 1 m, about 82 percent of the same area is viewed. The coincident area for all three bands is about 87 percent at 2 m, dropping to 74 percent at 1 m.

The greater tube separation of the Exotech 4-band causes a smaller coincident area than for the three-band. Figure 9B shows the ratio for two adjacent bands, two diagonal bands, and for all four bands for this instrument. At 2 m, the ratio is 85 percent, dropping to 70 percent at 1 m. The ratio for the four-band coincident area is 71 percent at 2 m and 47 percent at 1 m.

We have considered only the height perpendicular to a flat target. In a field, the soil surface is considered the flat target, and the radiometer is held vertically a distance h above the soil. Plants, protruding above the surface, alter the picture somewhat. Consider a situation in a field where the radiometer is held 2 m above the soil surface. If plants are in the scene, the coincident area will be less for the tops of the plants than at the soil surface. Figure 10 shows a side view and a top view of what a single band (15° FOV) radiometer "sees" when held 2 m above the soil surface. The centers of the plant rows (designated by the horizontal lines) are 0.3 m apart (approximately the row spacing of wheat in the northern Great Plains), the row width is 0.1 m and the plant height is 0.2 m.

At 2 m, a 15° FOV radiometer will see portions of 1-1/2 rows of plants, depending upon where the radiometer was located above the row. Depending upon location, it is possible that the radiometer could view most of two plant rows in one instance and only slightly over one row in another. Since it is difficult to hand-hold a radiometer much higher than 2 m, it is necessary to take a series of measurements at various horizontal locations (maximum height) across the rows in order to get an adequate sample of the reflectance properties of the entire plot. This problem can be reduced by increasing the field of view of the instrument; however, the danger exists of getting portions of the operator's body in the radiometer scene. Figure 11 depicts this possibility in the form of a person standing on a plank (to increase radiometer height) holding a radiometer. Two fields of view, 15° and 24°, are shown. The edge of the 24° scene is about 20 cm from the plank. The radiometer is shown level. In practice, it is very difficult to hold a radiometer sufficiently level to guarantee no "foreign" bodies in the scene. Furthermore, the total field of view is usually somewhat larger than that specified by the manufacturer. Peripheral

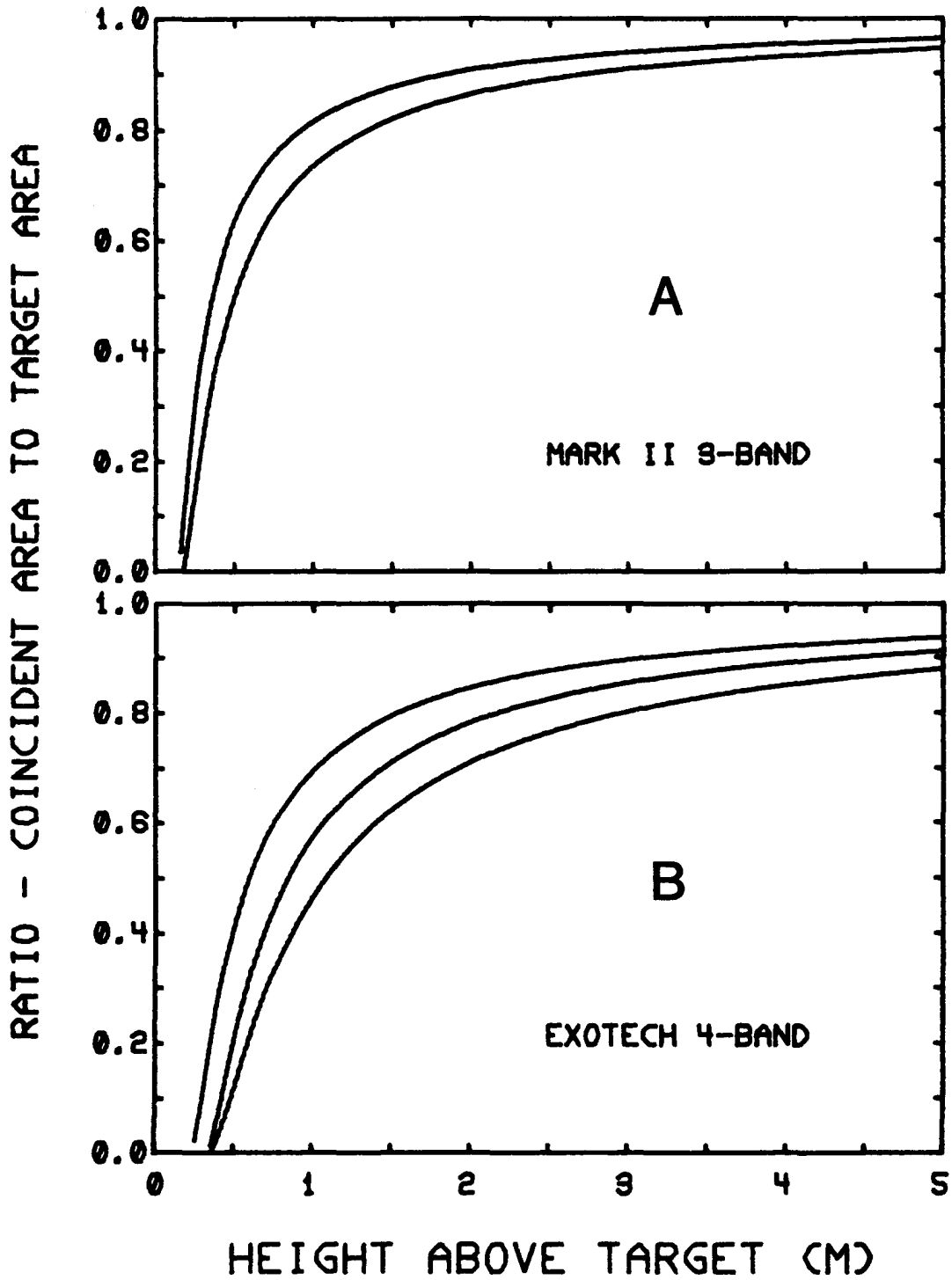


Figure 9.--Ratio of coincident area to target area versus height above target for a three-band and a four-band radiometer. For the Mark II 3-band, the upper line considers any two of the three bands and the lower line considers the coincident area for all three bands. For the Exotech, the upper line is for two adjacent bands, the middle line is for two diagonal bands, and the lower line is for all four bands.

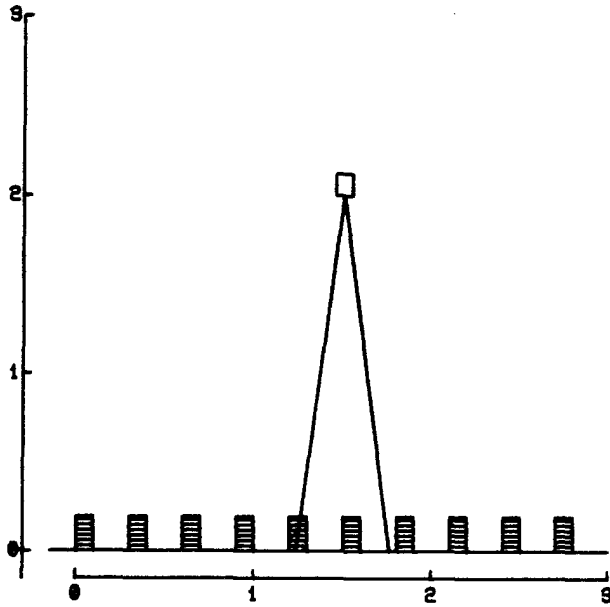


Figure 10.--Side and top views of a 15° FOV single band radiometer.  
The scale is in meters.

regions outside of the target area influence the radiance measurements because the angles of acceptance of the lenses are not sharply defined.

### RADIOMETRIC PLANT COVER

The concept of radiometric plant cover originates from the geometric fact that the side as well as the top of an object protruding above a surface will be seen if viewed from an angle. Furthermore, the object will obscure part of the surface as viewed from a radiometer. If the object is a row of plants, more vegetation and less soil will be seen as the view angle increases. Jackson et al. (1979) developed a model that calculates the fractions of soils, plants, and their shadows, as seen by an airborne scanner viewing across plant rows. We have used a similar approach to develop a model (details will not be presented here) for the circular view from a hand-held radiometer. The model assumes that plant rows can be approximated by rectangular blocks. We will present some calculated results to demonstrate how the fraction of plant cover seen by the radiometer may change when the radiometer height is changed, the plants grow, the row spacing is changed, and the degree of actual plant cover is changed. The "actual" plant cover is the fraction of plant material that covers the ground. It is the row

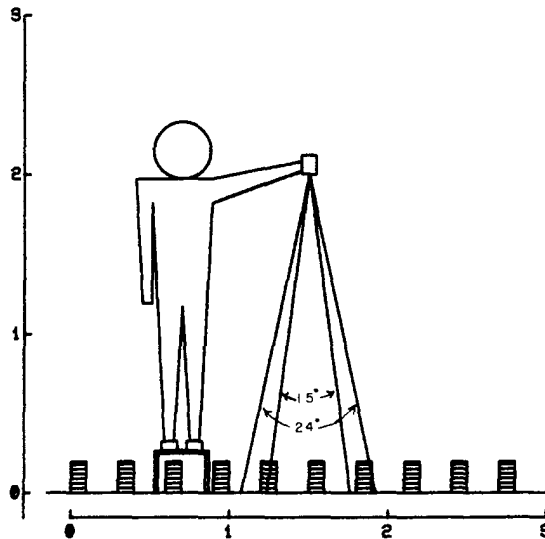


Figure 11.--Side view of an operator holding a radiometer. Two fields of view are shown. The inner two lines are for a 15° FOV and the outer two for a 24° FOV. The scale is in meters.

width divided by row spacing. In this case, plant height is not a factor. The actual plant cover will serve as a reference by which to compare the "radiometric" plant cover.

As noted earlier, the radiometric plant cover will depend on the position of the radiometer with respect to row structure. The extreme situations are when the lens is directly over the center of a plant row and when it is directly over the center of the exposed soil. We calculated what a radiometer would see at these extremes for various values of radiometer height above the soil surface for several plant heights, row spacings, row widths, and for two fields of view (15° common to both the Exotech and the Mark II and the 24° of the Mark II). Figure 12 shows a side and a top view of a radiometer held at heights of 1, 2, and 3 m. In the top view, the inner circle represents the view from 1 m; the middle circle, the view from 2 m; and the outer circle, the view from 3 m. Examination of this figure shows how the relative fractions of soils and plants change with changes in radiometer height. Subsequent figures in this section will show only the relative fraction of plant material in the scene of a radiometer held at two locations as the radiometer is raised from 0.5 to 5 m.

Case 1, row spacing = 0.3 m, row width = 0.15 m, FOV = 15°: Figure 13 shows the radiometric plant cover as related to radiometer height for zero plant height. This fictitious situation shows the symmetry of the fraction of plant cover viewed by the radiometer when held over the plant row and over the soil. The average of the two lines would be the actual plant cover (designated by the dashed line). The symbols merely identify the lines, the circles designate the view over a plant row, and the crosses represent the view over the soil surface. Notice how the lines crisscross as height is increased. At about 1.75 m, about 40-percent plant cover is observed when the radiometer is centered over the plant row and about 60 percent when centered over the soil. The amplitudes of the swings decrease with height but are still observable at 5 m. The significance

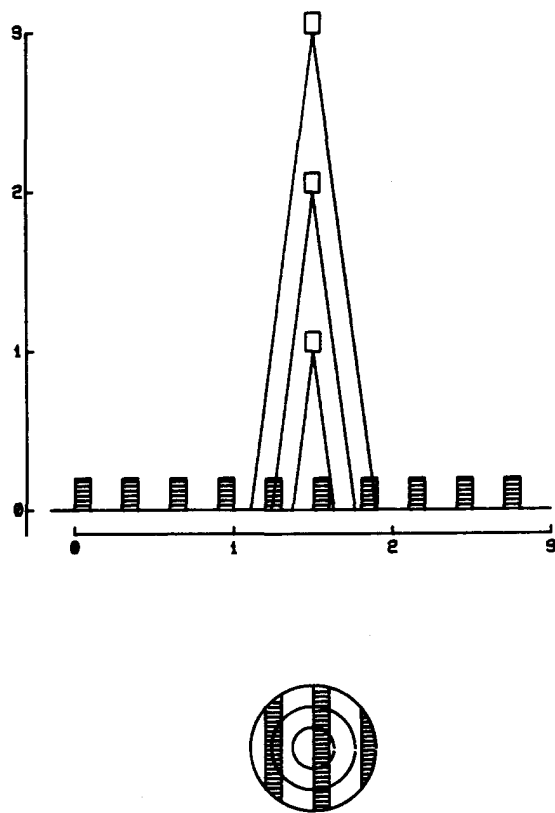


Figure 12.C-Side and top views of a 15° FOV radiometer held at three heights. The scale is in meters.

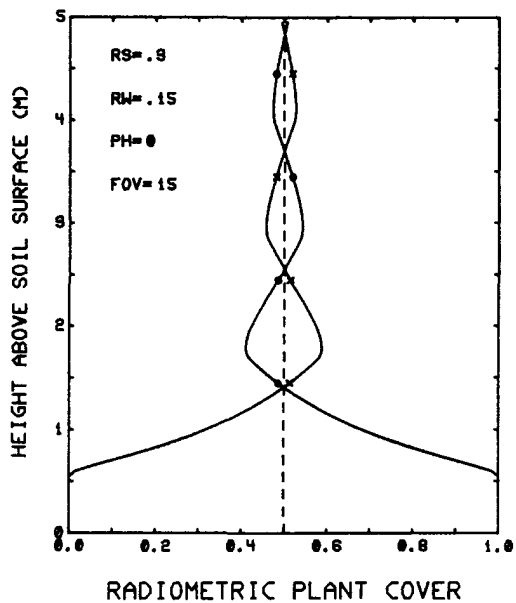


Figure 13.--Radiometric plant cover as a function of height above soil surface for a radiometer held over the plant row (circles) and over the exposed soil (crosses), for a 15° FOV instrument, plant height/width ratio is zero.

of the proportion between plants and soil becomes clear when one considers that the reflectance of soil in the visible (red) region may be as much as 10 times that of green plant material.

Figure 14 shows results of calculation for a plant height/width ratio of 1, i.e., a plant height of 0.15 m. Note the asymmetry of the two lines. The average of the two would yield a radiometric plant cover of about 53 percent as compared with the actual of 50 percent. Figure 15 shows similar results for a 2:1 height/width ratio. The degree of asymmetry increases, and the average radiometric plant cover becomes about 56 percent. When the height is increased to 0.45 m, a 3:1 ratio, the asymmetry is greater (fig. 16). After the first cross over, the lines never go below the actual plant cover line (dashed line), and the average at 5 m is about 58 percent.

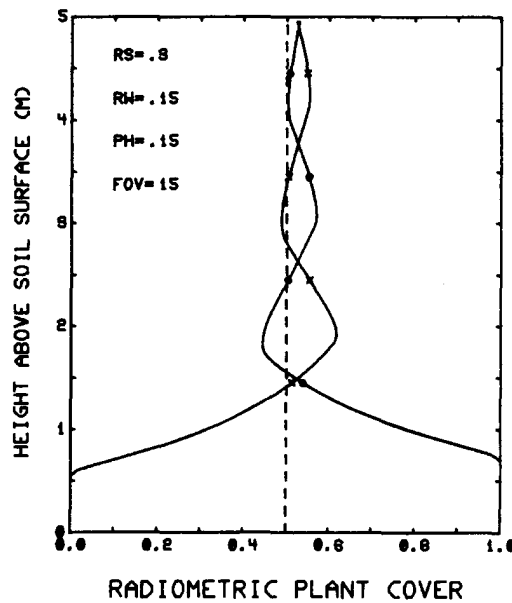


Figure 14.--Same as figure 13 except plant height/width ratio is 1.

Case 2, row spacing = 0.3 m, row width = 0.15 m, FOV = 24°: When the field of view is increased, a radiometer will see more vegetation. Figure 17 shows the situation for 1:1 height/width ratio and 24° FOV. The same pattern holds as did in figures 13 to 16, but the amplitude of the swings is less and the radiometric plant cover is greater (about 55 percent). Increasing plant height to a 2:1 ratio yields an average radiometric cover of nearly 60 percent (fig. 18), and a 3:1 ratio (fig. 19) is about 63 percent.

The lower amplitude of the swings would indicate the desirability of increasing the FOV of the radiometers; however, this increases the bias towards plants and the larger field of view may cause the operator's feet or other out-of-target materials to be viewed (see discussion in previous section).

Case 3, row spacing = 1 m, row width = 0.5 m, FOV = 15°: This case is representative of plants such as cotton and corn. Figure 20 shows calculations

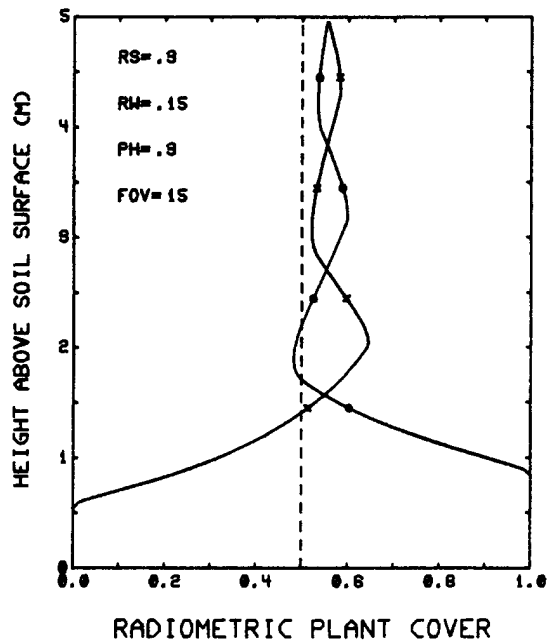


Figure 15.--Same as figure 13 except plant height/width ratio is 2.

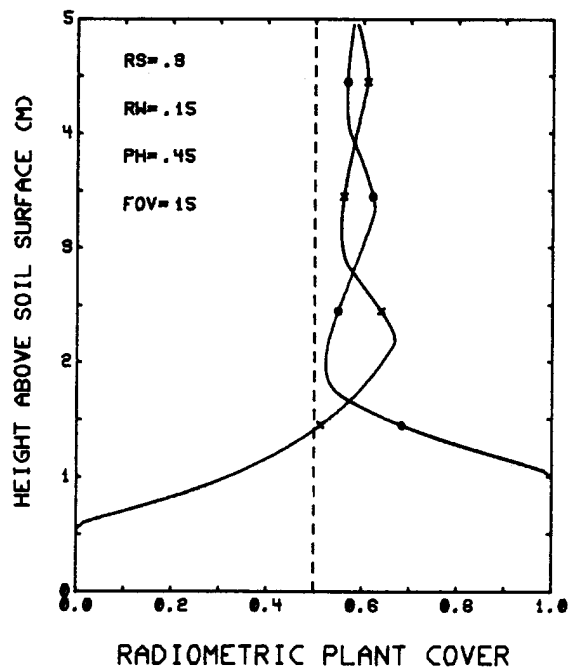


Figure 16.--Same as figure 13 except plant height/width ratio is 3.

for a plant height of 1 m, and a 2:1 height/width ratio. This situation is similar to a cotton crop in June in Arizona. Obviously, adequate data could not be obtained with an operator standing on the soil holding a radiometer. It would be preferable to have the instrument above 5 m. Figure 21 shows calculations for a 3:1 ratio, somewhat representative of corn. Apparently, adequate

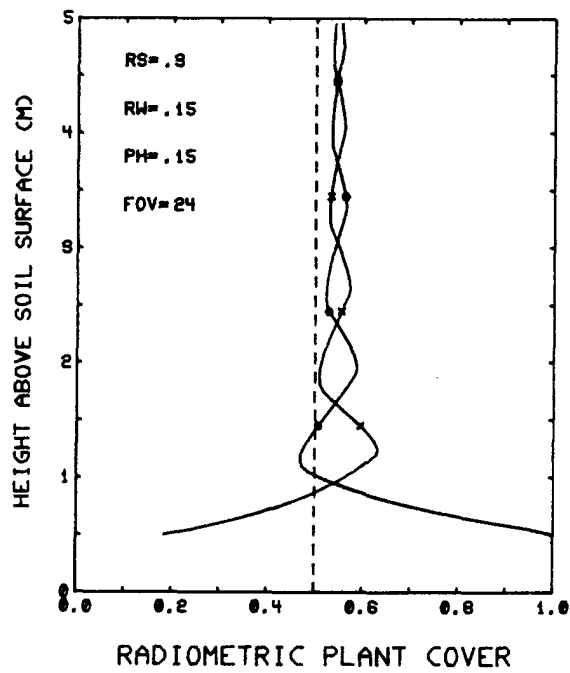


Figure 17.--Same as figure 13 except 24° FOV, plant height/width ratio of 1.

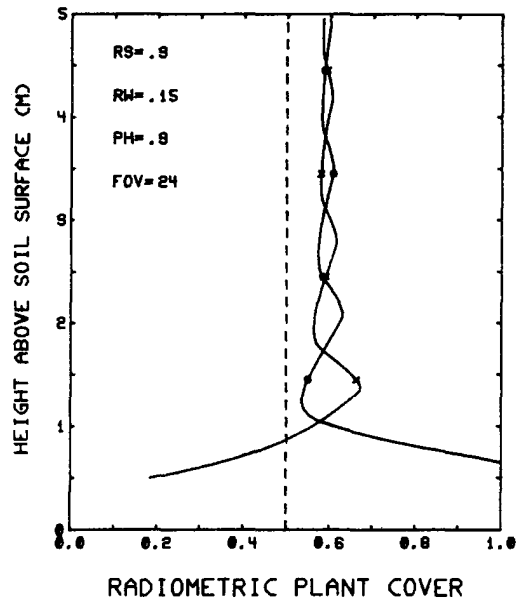


Figure 18.--Same as figure 13 except 24° FOV, plant height/width ratio is 2.

data could not be obtained unless the radiometer was held considerably higher than 5 m.

The asymmetry shown in figures 20 and 21 indicates that taking a reading over a row and another over the furrow and averaging the two may not yield a

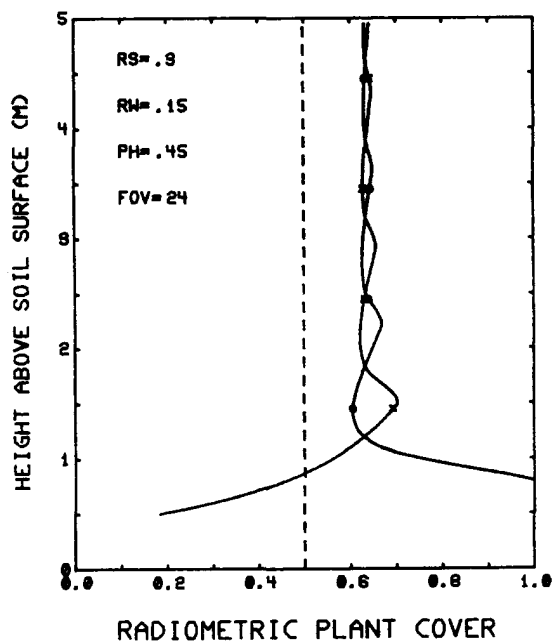


Figure 19.--Same as figure 13 except 24° FOV, plant height/width ratio is 3.

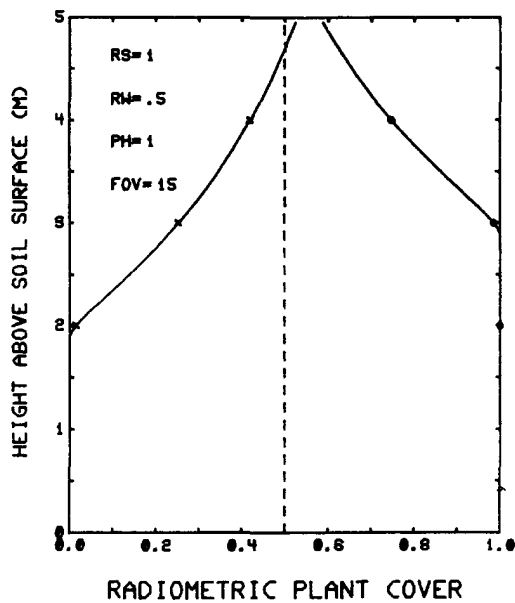


Figure 20.--Radiometric plant cover versus radiometer height above soil surface for a 15° FOV instrument. Row spacing 1 m, plant height 1 m, row width 0.5 m, conditions similar to cotton in June in Arizona.

sufficiently accurate value for the composite scene. A more appropriate scheme may be to take a number of readings as the radiometer is moved from over the row to over the furrow. The higher the plants and the wider the row spacing, the more care must be used in making the measurements and in interpreting the data.

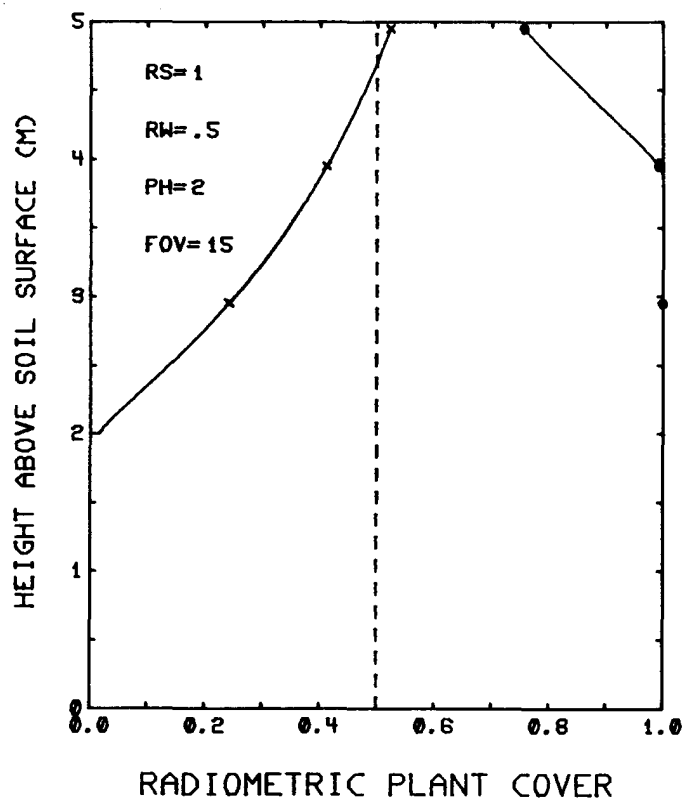


Figure 21.--Same as figure 20 except plant height is 2 in, height/width ratio of 3, conditions similar to a corn crop.

### VEGETATION INDICES

A spectral vegetation index is a quantity obtained directly or by ratioing, differencing, or otherwise transforming spectral data to represent plant canopy characteristics such as leaf area index, biomass, green weight, dry weight, per cent cover, and so on. This definition was furnished by Craig Wiegand in a letter dated 9 May 1978. In addition, his letter contained comments that are very pertinent to the subject of this workshop. These comments (edited somewhat to fit into this discussion) are represented in the following paragraph.

There appears to be a growing confusion in the literature and in conversations with individuals over what a given person means when the words "vegetation index" are used. Until recently, most spectral data in the literature came from LANDSAT investigations. Now, however, results are becoming available from the NASA field measurements program (truck, helicopter, and aircraft mounted devices) and from hand-held radiometers such as those used by Jim Tucker at NASA/GSFC and some SEA/AR groups. Some LANDSAT investigators routinely adjust readings for seasonal and sun angle variations, and some locations, such as the Environmental Research Institute of Michigan (ERIM), have the capability for adjusting the data for atmospheric attenuation. Thus, both investigators, sensors, and the number of "indices" are proliferating. To reduce the confusion, authors can:

- (1) Mention the specific wavelengths and describe the sensor system used.
- (2) Clearly indicate whether incident light, reflectance standards, or other normalizations are used.
- (3) Describe any preprocessing of the raw data before it was used to calculate the spectral parameters.
- (4) Mathematically express the particular parameter(s) calculated at least once in reports or manuscripts.

We strongly concur with Wiegand's comments. The following discussions of ratios, normalized differences, and other band combinations to yield vegetation indices hopefully will help to reduce confusion. For other discussions of vegetation indices, see Richardson and Wiegand (1977) and Tucker (1979).

Ratios: The ratio of radiance or reflectance values from two bands is a simple and useful vegetation index, if the bands are properly chosen. One criterion for choosing two bands for a ratio vegetation index is that data from one band should decrease with increasing green vegetation in the scene, and data from the other band should increase with increasing green vegetation.

Figure 22 shows spectral data from 0.43 to 1 micrometer obtained by Ungar et al. (1977), using an aircraft mounted spectrometer. Data for a bare soil field and for an alfalfa field are given in the same figure to show the difference in spectra between the two. The alfalfa line is interrupted as it crosses the soil line for clarity of presentation. Consider these plots only as representative samples. Spectra for other soils, crops, and even other alfalfa fields may be somewhat different; however, the general shape will be the same. The ordinate is in units of radiance, but the specific values are not pertinent to this discussion. Of importance here are the relative differences between soils and plants as the wavelength is changed.

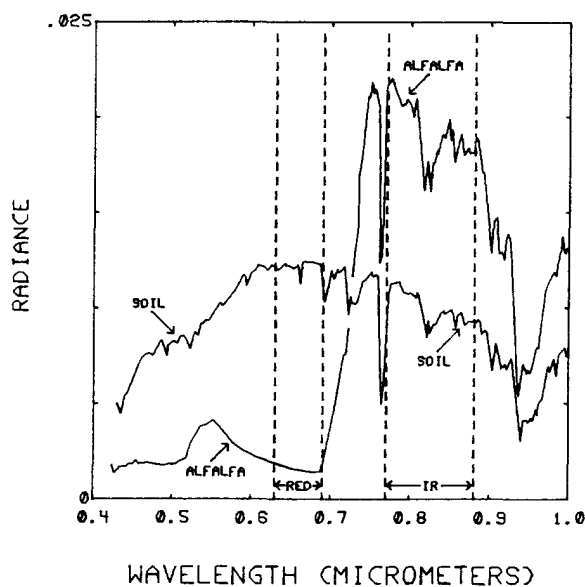


Figure 22.--Soil and alfalfa spectra (data of Ungar et al. 1977). The dashed lines indicated by "red" and "IR" show the red and IR bands of the Mark II hand-held radiometer.

Starting at about 0.43  $\mu\text{m}$ , the soil spectrum increases to a maximum at about 0.65  $\mu\text{m}$  and then slowly decreases to a minimum at about 0.94  $\mu\text{m}$ . The alfalfa spectrum starts below the soil, has a small peak near 0.55  $\mu\text{m}$ , then decreases to a minimum at about 0.69  $\mu\text{m}$ , followed by a sharp increase (becoming almost twice as high as the soil spectrum), reaching a maximum at about 0.75  $\mu\text{m}$ . Above 0.75, the alfalfa spectrum declines but does not go below the soil spectrum.

The band between 0.63 and 0.69  $\mu\text{m}$  is known as the chlorophyll absorption band and is shown by dashed lines at 0.63 and 0.69  $\mu\text{m}$  in figure 22. Tucker (1979) reviewed the various wavelength regions with respect to their sensitivity for monitoring vegetation. Within this band, the soil radiance is at a maximum and plant radiance is at a minimum. This indicates that a band within the red portion of the visible spectrum is a sensitive indicator of green vegetation. Figure 22 shows that the plant spectrum is almost double the soil spectrum within the range of about 0.75 to 0.9  $\mu\text{m}$  (photographic IR, fig. 4). The IR band of the Mark II radiometer is indicated by the second set of dashed lines (0.77 to 0.88  $\mu\text{m}$ ). Thus, a band in this region would also be sensitive to vegetation. The ratio of a band that increases with increasing vegetation (near IR) to a band that decreases with increasing vegetation (visible red) yields a parameter that is highly sensitive to vegetation. A history and a discussion of the IR/red ratio is given by Tucker (1979).

The above discussion points out advantages of using an IR/red ratio. Actually, ratios can be calculated for any two bands. A second reason for using a ratio as a vegetation index is that radiance measurements can be used directly, without converting to reflectance by ratioing with radiance values from a standard reflectance plate. In some cases, the instrument voltages are ratioed; however, this makes a comparison of data from different instruments difficult because calibration factors may be different. This can be seen by writing equation 2 for bands, designated as a and b, and ratioing, i.e.,

$$L_a/L_b = (C_a/C_b)(V_a/V_b) \quad (15)$$

The radiance ratio differs from the voltage ratio by the factor  $C_a/C_b$ . Usually, the calibration factor for one band is not very different from the other; however, if calibration constants are known, it is preferred to form the product CV for each band before ratioing.

The ratio of the radiances of two bands may differ from the ratio of the reflectances of the same two bands. Again using the subscripts a and b to denote the two bands, and using equation 3, we have

$$L_a/L_b = (E_a/E_b)(R_a/R_b) \quad (16)$$

With equation 4, we can also obtain the irradiance from measurements on a standard reflectance plate. We have

$$E_a = L_{ap}/R_{ap} \quad (17)$$

and 
$$E_b = L_{bp}/R_{bp} \quad (18)$$

forming the ratio  $E_a/E_b$  using equations 17 and 18 and substituting into

equation 16 yields,

$$L_a/L_b = [(L_{ap}/R_{ap})/(L_{bp}/R_{bp})](R_a/R_b) \quad (19)$$

Thus, the ratio of the radiance will equal the ratio of the reflectance only when the radiance measured over a standard reference plate (at very close to the same time as the radiances over the target are measured) is equal in the two bands and when the standard plate reflectances for the two bands are equal.

We therefore extend Wiegand's comments to include a request that, when ratios are reported, the means of obtaining the ratios be specified (i.e., voltage ratios, radiance ratios, or reflectance ratios).

Normalized difference: A normalized difference is a ratio of the difference between values for two bands and the sum of the values for the two bands. This ratio was developed as a vegetation index by Don Deering and Bob Haas during a LANDSAT-1 rangeland study and was discussed by Rouse et al. (1973), Deering et al. (1975), and Deering (1978). They used the LANDSAT IR and red channels to form the difference ratio and named this ratio the Vegetation Index, i.e.,

$$VI = (IR - Red)/(IR + Red) \quad (20)$$

Subsequently, as more researchers became involved and more data became available, the term "Vegetation Index" became applied to almost all band combinations used as a measure of vegetation. Deering (1978) has since proposed that this index be named the Normalized Difference (ND). We concur and will use this term in subsequent discussions; however, we will not restrict our definition of the ND to the red and IR bands, but will use it as a general term for any two band difference/sum ratio.

Writing the ND in terms of radiance, we have

$$ND = (L_a - L_b)/(L_a + L_b) \quad (21)$$

We see that, as with the ratio, it should be clearly stated what bands are used, and whether the input data are voltages, radiances, or reflectances. It is left as an exercise for those interested to use the relation  $L = CV$  in equation 21 and to show that a different value of ND will obtain if reflectances are used instead of radiances.

Transformed ND: For scenes in which the vegetation density is low, ND may become negative. This can be seen by examination of figure 22. For very low vegetation densities, the radiance will be nearly that of the soil. In this case, a band in the red region will have a larger value than a band in the IR, and the differences will be negative. To avoid the negative values and to minimize some possible statistical problems, a constant 0.5 was added to the normalized difference and a square-root transformation was applied. Thus,

$$TND = (ND + 0.5)^{1/2} \quad (22)$$

was defined, and is known as the transformed ND. As a reminder, the terminology "Normalized Difference" is relatively new. Most of the literature uses the terms "Vegetation Index" and "Transformed Vegetation Index."

Numerical example: The above discussion indicates that ratio and difference ratio vegetation indices may not be the same for indices calculated using radiance values and those calculated using reflectance values. The degree of difference can readily be seen using some actual values that were obtained during a field experiment using an Exotech model 100A hand-held radiometer. The radiance data shown in table 1 were taken over a wheat plot at 1135 MST on 1 February, 1980. Twelve measurements were made over the plot and 12 were made over a BaSO<sub>4</sub> plate immediately after (within one minute). The raw data were averaged and converted to radiances using equation 15 and the calibration factors supplied by the instrument manufacturer. Values for the BaSO<sub>4</sub> plate reflectance (R<sub>p</sub>) were for a plate loaned to us by LARS, Purdue University. The actual plate used in these experiments was constructed in a similar manner to the LARS plate; however, the true values of R<sub>p</sub> may differ. For this discussion, the absolute value of the plate reflectance is not important. The concepts involved will not be altered by a small difference in the numbers.

Table 1. B-Spectral data taken over a wheat plot and a BaSO<sub>4</sub> reflectance plate, using an Exotech model 100A hand-held radiometer

	Spectral band			
	MSS4 (0.5 to 0.6)	MSS5 (0.6 to 0.7)	MSS6 (0.7 to 0.8)	MSS7 (0.8 to 1.1)
Target radiance (L <sub>t</sub> ) (w/m <sup>2</sup> )	3.75	4.12	21.11	39.97
BaSO <sub>4</sub> plate radiance (L <sub>p</sub> )(w/m <sup>2</sup> )	75.12	92.01	72.68	95.98
BaSO <sub>4</sub> plate reflectance (R <sub>p</sub> )	0.943	0.942	0.941	0.937
Target reflectance (R <sub>t</sub> )	0.047	0.042	0.273	0.390
Irradiance (I = L <sub>p</sub> /R <sub>p</sub> )(w/m <sup>2</sup> )	79.66	97.68	77.24	102.43

Irradiance values were calculated using equations 17 and 18. The data in table 1 were used to calculate ratios and normalized differences for several two-band combinations of the four bands of the Exotech. These data are presented

in table 2. In the table, the bands are assigned the letters a and b to facilitate their use in equations 16 and 21.

Two visible bands, such as MSS4 and MSS5, are not often used to calculate vegetation indices; however, the results in table 2 show that, if used, the radiance and reflectance ratios may differ by about 20 percent, and the ND even changes sign. The bands MSS6 and MSS5 can be considered as IR and red. The ratio MSS6/MSS5 is 27 percent different when radiances rather than reflectances are used. The ND is about 9 percent different. MSS7 and MSS5 are two frequently used bands for calculating the ratio and the ND. These bands show less than 5 percent difference for the ratio, and the ND has less than 1 percent difference.

Table 2.--Band ratios and normalized differences calculated using radiance ratios and reflectance ratios of spectral data obtained over wheat with an Exotech model 100A hand-held radiometer. The symbols L and R indicate that values used for the indices were radiance and reflectance, respectively

Band combination used in equations 16 and 21	Ratio		Normalized difference	
	L	R	L	R
a = MSS5, b = MSS4	1.10	0.89	0.047	-0.06
a = MSS6, b = MSS4	5.63	5.81	.698	.706
a = MSS7, b = MSS4	10.66	8.30	.828	.785
a = MSS6, b = MSS5	5.12	6.50	.673	.733
a = MSS7, b = MSS5	9.70	9.29	.813	.806

Examination of equations 17, 18, and 19 shows that the radiance ratio differs from the reflectance ratio mostly by the ratio of the irradiance of the two bands. The irradiance values shown in table 2 are, therefore, the key to the differences observed. Irradiance values of MSS5 and MSS7 are not very different from each other but are quite different from values of MSS4 and MSS6. The use of MSS5 and MSS7 in vegetation indices would not show much difference whether radiance or reflectance values were used. Combinations of bands that show quite different irradiance values will exhibit the largest difference between those values calculated with radiances and reflectances.

This example underscores the need for carefully describing how various indices are calculated and shows that the irradiance is not the same in every band. This latter point plays a role when data obtained from instruments with different band widths are compared.

Perpendicular Vegetation Index: In addition to ratios and difference ratios, many other combinations of spectral bands have been used as vegetation indices. The Perpendicular Vegetation Index (PVI) of Richardson and Wiegand (1977) stands out among these. The development of the PVI follows many of the arguments used by Kauth and Thomas (1976) to produce the "tasseled cap" model of vegetation development. Whereas Kauth and Thomas used vector analysis in four dimensional space to produce a tasseled cap (a plot of the data looks like a tasseled cap), Richardson and Wiegand used algebraic relations in two dimensions. Both groups used LANDSAT data as the basis for their developments.

We will use a two dimensional approach similar to that of Richardson and Wiegand (1977). Kauth and Thomas (1976) and Richardson and Wiegand (1977) showed that a plot of LANDSAT digital data from bare soil fields of MSS7 (IR) versus MSS5 (red), or MSS6 (IR) versus MSS5 (see fig. 4 or table 1 for wave length regions corresponding to these band numbers) yielded a straight line. Richardson and Wiegand commented that the soil line appeared constant from one overpass date to another and that the intercept was not significantly different from zero. This comment indicates that the soil line may be constant for various soils and that wet and dry soil would fall on the same line. When vegetation covers part of the soil, reflectances in the red band will decrease and the IR will increase (for most soils). This is shown schematically in figure 23. Point C represents data containing vegetation but with some soil background showing. The PVI is the perpendicular distance from the soil line to the point in question. To calculate this distance, an equation for the soil line is needed. We define Y as a band in the IR (it can be MSS6 or MSS7 or the Mark II IR band), and X as a band in the visible (usually in the red region, MSS5 or the Mark II red band). The soil line is

$$Y = a_0 + a_1X \tag{23}$$

The coefficients  $a_0$  and  $a_1$  are found by linear regression of data taken over bare soils. To find the distance from a line to a point, reduce the equation of the line to normal form and substitute the coordinates of the point in the equation (Rider, 1947), i.e.

$$PVI = (Y_i - a_1X_i - a_0)/[1^2 + (-a_1)^2]^{1/2} \tag{24}$$

where the subscript i indicates that  $X_i$  and  $Y_i$  are coordinates of a point not on the soil line, which for convenience is called a vegetation point.

Figure 23 shows a soil line and five points representing measurements over soils and vegetated surfaces. Points A and B represent bare soil data. Point A represents the highly reflective dry soil, whereas point B represents the less reflective wet soil. (A rough surface that produced microshadows would have a similar effect.) Data for soils at intermediate water contents would fall between points A and B on the soil line. It is possible, in theory, to calibrate a point on the line as to its water content. In practice, a quantitative scale would be difficult to develop, but qualitative measures of wet, medium, and dry evaluations of the surface soil may be practical for some soils.

Points C and D in figure 23 are representative of data taken over a vegetated field having about 25 percent plant cover. Point E represents a location with essentially 100 percent plant cover. From figure 22, we see that the red

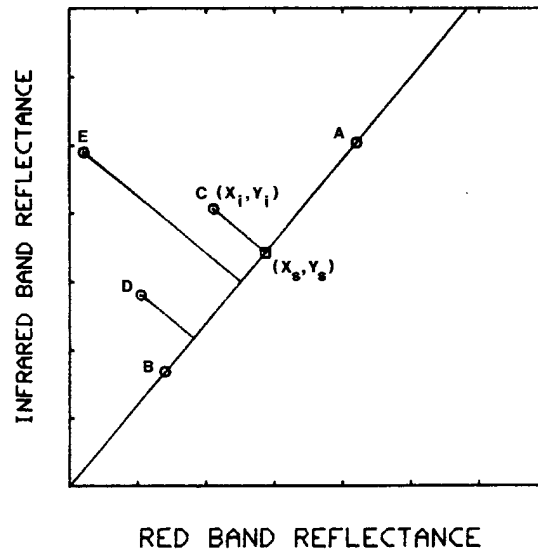


Figure 23.--Diagram of the soil line and vegetation points for use in calculating the Perpendicular Vegetation Index.

band decreases and the IR band increases as one goes from soils to vegetation. Points C and D represent the same amount of vegetation yet plot quite differently on the graph. This case demonstrates the strength of the PVI as a vegetation index. The points plot differently, but both are the same distance from the soil line and therefore would have the same value for the PVI. This situation could arise by taking a measurement over the field when the soil was dry (point C), irrigating the field, and repeating the measurement when the soil was wet (point D). At point E (100 percent cover), no effect on spectral measurements would be observed by the soil surface changing from wet to dry. In theory, the PVI removes the effect of soil background. The point on the soil line where the perpendicular line to the point originates gives some information about soil conditions (if, for the particular soil, the wet and dry end points on the soil line are known), but only in proportion to the amount of soil viewed. Richardson and Wiegand (1977) developed the PVI in terms of the coordinates on the soil line, allowing them to obtain values for the soil reflectance in the vegetation-soil scene.

Obtaining the coordinates of the point on the soil line where the line from the vegetation point is perpendicular requires a little review of algebra and geometry. The equation for the soil line is  $Y = a_0 + a_1X$ . Let the line from a vegetation point to the soil line be  $Y = b_0 + b_1x$ . At the point of intersection of the two lines, the values of Y and the values of X will be the same. Thus, the two equations are solved simultaneously for K and Y. We equate

$$a_0 + a_1X_s = b_0 + b_1X_s \quad (25)$$

and solve for  $X_s$ , yielding

$$X_s = (b_0 - a_0)/(a_1 - b_1) \quad (26)$$

where the subscripts indicate that the coordinates are on the soil line.

Writing the two equations with X as the dependent variable and solving for  $Y_s$  yields

$$Y_s = (a_1b_0 - a_0b_1)/(a_1 - b_1) \quad (27)$$

The point  $(X_s, Y_s)$  is represented by a square symbol in figure 23. Equations 26 and 27 are essentially the same as equations 5 and 6 of Richardson and Wiegand (1977). (We chose to put the IR band as the ordinate and the red band on the abscissa in our development, opposite to the way Richardson and Wiegand labeled theirs. Both ways are correct.)

We now have values for the coordinates at the vegetation point  $(X_i, Y_i)$  and at the intersection of the perpendicular on the soil line  $(X_s, Y_s)$ . Using the Pythagorean Theorem, we can solve for the distance between the two points, i.e.,

$$PVI = [(Y_i - Y_s)^2 + (X_i - X_s)^2]^{1/2} \quad (28)$$

which is an equivalent form of the PVI developed by Richardson and Wiegand (1977) (their equation 4). If only the PVI is of interest and information on soil background is not required, equation 24 requires less computation. If the point on the soil line is of interest, then equations 26 and 27 need to be solved. The slope of the vegetation line ( $b_1$ ) is equal to  $C1/a_1$  because the two lines are perpendicular. The intercept of the vegetation line ( $b_0$ ) is  $Y_i + (1/a_1)X_i$ . The coordinates for the intersection with the soil lines are

$$X_s = (a_1 Y_i + X_i - a_0 a_1) / (a_1^2 + 1) \quad (29)$$

$$Y_s = (a_1^2 Y_i + a_1 X_i + a_0) / (a_1^2 + 1) \quad (30)$$

Equations 29 and 30 give the soil line coordinates for the perpendicular to the vegetation point in terms of the coordinates of the vegetation point and the coefficients of the equation for the soil line.

In this development of PVI, the equations have deliberately been left in terms of unevaluated coefficients. An interested person can choose a particular visible band (preferably in the red region) for the X and a near IR band for the Y, determine the soil line (and thus the coefficients  $a_1$  and  $a_0$ ), and utilize the PVI. Richardson and Wiegand's development was in terms of radiances in specific LANDSAT MSS bands.

The soil line: The soil line is basic to the PVI of Richardson and Wiegand (1977) and to the tasseled cap of Kauth and Thomas (1976). The assumptions are that the soil line is linear and all soils yield data that fall on the line. Adequate tests of these assumptions using LANDSAT data would require a considerable amount of ground data collection and computer time. Hand-held radiometer data can be used advantageously in this case to provide an insight as to the validity of the assumption.

At the U.S. Water Conservation Laboratory at Phoenix, measurements of dry and wet bare soil are a routine part of the spectral measurements program. Data for the 1979 season (139 data points) are shown in figure 24. Regression analysis indicates that a linear relation is a good representation of the data ( $r^2 = 0.98$ ), supporting the assumption of linearity in the development of the PVI.

$$PVI = 0.647Y - 0.763X - 0.020 \quad (31)$$

Using the regression coefficients shown in figure 24 in equation 24 yields Where Y refers to the MSS7 reflectance and X to the MSS5 reflectance.

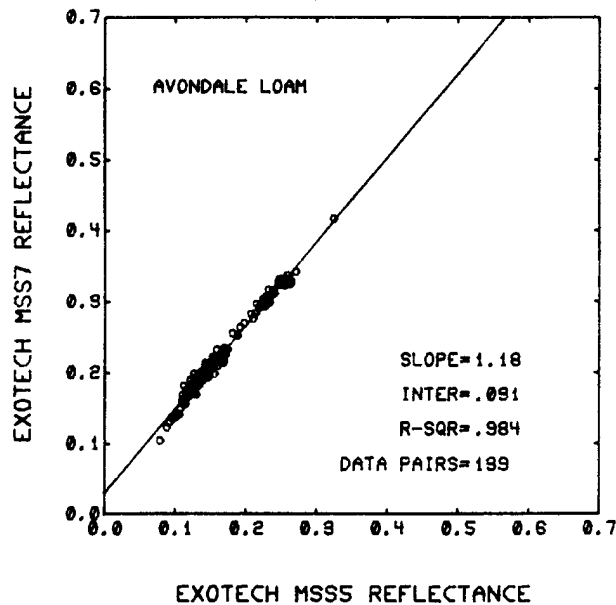


Figure 24.C-The soil line (bare soil data) using red (MSS5) and infrared (MSS7) bands. Data taken with an Exotech model 100 hand-held radiometer.

The data were all taken while the soils were sunlit. In a plant canopy, portions of the soil viewed by a radiometer may be shaded. Data for shaded soils would fall close to the origin and probably would not be represented by the extrapolation of the linear line to the point of intersection with the ordinate. This situation needs additional study.

Some insight into this situation, and the assumption that different soils will fall on the same line, can be gleaned from figure 25, where data for eight different porous materials are shown. In the following discussion of symbols, the coordinates (X, Y) of the wettest and driest data points for these measurements are given. The circular symbols (25 of the 40 data pairs) furnished by J. K. Aase<sup>3</sup> are for Williams loam near Sidney, which has reflectance coordinates that range from (0.065, 0.119) to (0.229, 0.313). Three crosses represent wet and dry Avondale loam, a light-colored soil from near Phoenix whose reflectance coordinate range was (0.123, 0.193) to (0.275, 0.353). Two plus symbols represent a red-colored soil, coordinates (0.080, 0.124) and (0.091, 0.150), that had the smallest range of all. Two square symbols represent a light, reddish soil, coordinates (0.147, 0.205) and (0.271, 0.361). Two lazy diamond symbols represent a mixture of Avondale loam and a silica sand, coordinates (0.151, 0.210) and (0.313, 0.403). Two inverted triangles represent a Superstition sand from near Yuma, Ariz., coordinates (0.283, 0.334) and (0.404, 0.446). Two triangles represent a white silica sand, coordinates (0.457, 0.547) and (0.583, 0.661). Two diamonds represent black cinders from near Flagstaff, Ariz., coordinates (0.023, 0.030) and (0.064, 0.077).

---

<sup>3</sup>Personal communication.

The data in figure 25 demonstrate the considerable range of reflectance values for different porous materials and also the range of reflectances for the same material when going from wet to dry (or vice versa). A conclusion that can be drawn is that the soil line is not linear over a wide range of soils and other porous materials. This is in contrast to figure 24, where the data were quite linear. We conclude that when an individual soil is considered and the range of data from wet to dry is determined for sunlit conditions, the data are sufficiently linear that the PVI can be used. Additional work is required to account for the nonlinear nature of the soil line when various materials are considered.

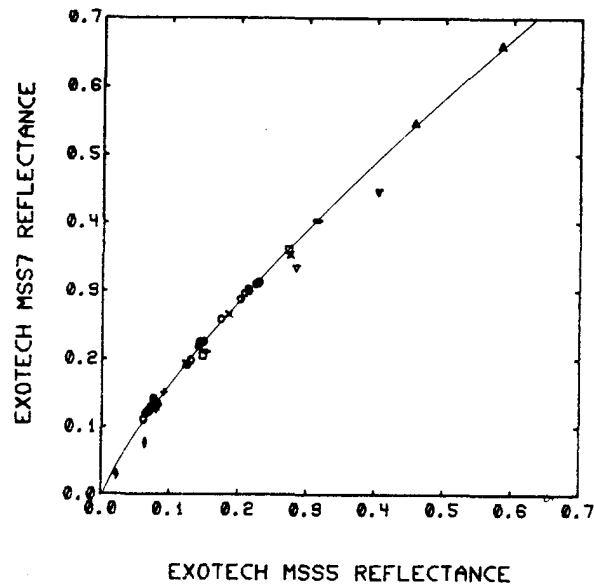


Figure 25.--The soil line for eight different porous materials ranging from black cinders to soils to white silica sand. The circular symbols represent Williams loam, data furnished by J. K. Aase, Sidney, Mont. Other symbols are discussed in the text.

Some readers may have noticed that we have used reflectances exclusively in this section. Radiances can be used, but since they are directly proportional to the irradiance their coordinates on a soil line will vary with sun angle. This is demonstrated in figure 26 where radiance values, taken at 10 time periods (spaced between 0800 and 1630 hours) during one day, are shown. At first glance, it is reassuring to see the linearity of the data; however, it can lead to the erroneous conclusion that both radiances and reflectances can be used directly in calculating the PVI.

Consider only the numerator in equation 24 (the denominator is a constant), i.e.,  $Y_i - a_1 X_i - a_0$ . If Y and X are in terms of radiance, a change in irradiance will change the PVI drastically, since the X and Y terms are of opposite sign. It is theoretically possible to overcome this problem by adjusting all X and Y values to constant irradiance levels.

Some calculated results: The purpose of obtaining vegetation indices is to gain information about vegetative growth. A question thus arises as to what

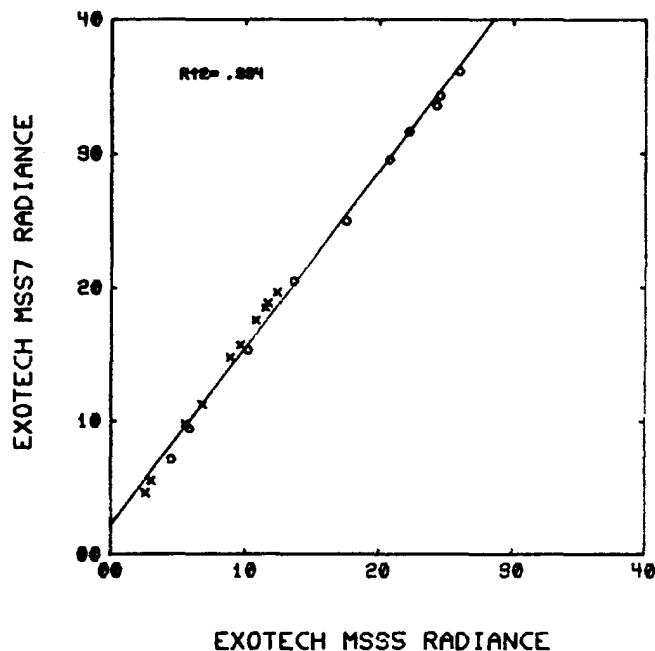


Figure 26.--The "soil line" for a set of diurnal measurements in terms of radiance. Circular symbols represent dry soil and crosses represent wet soil.

values of the several indices might be expected as a field changes from bare soil to full green vegetative cover. Although not considered here, the change from full green vegetative cover to completely senesced dry straw is of equal interest.

Wiegand et al. (1974), Richardson et al. (1975), and Jackson et al. (1979) discussed a linear model for calculating the spectral reflectance for composite scenes (scenes containing both soil and vegetation, sunlit and shaded). The model

$$R_c = f_{v1}R_{v1} + f_{vd}R_{vd} + f_{s1}R_{s1} + f_{sd}R_{sd} \quad (32)$$

can be written as

where  $R_c$  = composite scene reflectance,  $f_{v1}$  = fraction of sunlit vegetation,  $R_{v1}$  = reflectance of sunlit vegetation,  $f_{vd}$  = fraction of shaded vegetation,  $R_{vd}$  = reflectance of shaded vegetation,  $f_{s1}$  = fraction of sunlit soil,  $R_{s1}$  = reflectance of sunlit soil,  $f_{sd}$  = fraction of shaded soil, and  $R_{sd}$  = reflectance of shaded soil.

Data were taken with an Exotech hand-held radiometer over wet and dry bare soil and over a dense green sunlit wheat canopy. The measurements were repeated while the sun was blocked out over the target area to yield values for shaded reflectances. The red (MSS5) and one IR (MSS7) band of the Exotech were used. Reflectance values were for the red band:  $R_{v1} = 0.0256$ ,  $R_{s1}$  dry = 0.226,  $R_{s1}$  wet = 0.136,  $R_{sd} = 0.15 R_{s1}$ . Reflectance values for the IR band were  $R_{v1} = 0.535$ ,  $R_{s1}$  dry = 0.299,  $R_{s1}$  wet = 0.197, and  $R_{sd} = 0.11 R_{s1}$ . We assumed that all vegetation was sunlit, making the fraction  $f_{vd} = 0$ .

Calculations were made for four cases: sunlit vegetation and sunlit dry soil (a situation that would occur at solar noon), sunlit plants and sunlit wet soil (solar noon situation), sunlit plants and shaded dry soil, and sunlit plants and shaded wet soil. The latter two cases would occur for north-south plant rows during the morning hours if the plants are relatively tall. It is a somewhat fictitious situation at low values of plant cover; for low plant cover with completely shaded soil, the solar elevation would be so low that other problems would beset a reflection measurement.

Another caution that should be kept in mind about results calculated using equation 32 is that it is implicitly assumed that plants absorb or reflect the incident radiation and thereby produce shadows. This is a reasonable assumption in the visible region but does not hold for the IR. Some IR radiation is transmitted through plant leaves, making quite different "shadows" than we see with our eyes. Allen and Richardson (1968) have shown that IR radiation can penetrate eight layers of plant leaves before all the energy is reflected or absorbed. Wiegand et al. (1979) stated that the first leaf absorbs about 10 percent of the impinging light in the near IR with the remainder being divided equally between transmission and reflection. The light transmitted by the first leaves and the light that penetrates between the leaves interacts with lower leaves until it is completely attenuated at a leaf area index of 8. This complex interaction of the near IR and plants in the field requires some additional modeling.

With the above cautions in mind (but unaccounted for), we proceed to calculate the IR/red ratios, ND, and the PVI over the range of 0 to full green plant cover. Figure 27 shows results for the IR/red ratio. For the sunlit soil conditions (both wet and dry, representative of solar noon measurements), the ratio is not very sensitive to plant cover. For shaded soil conditions

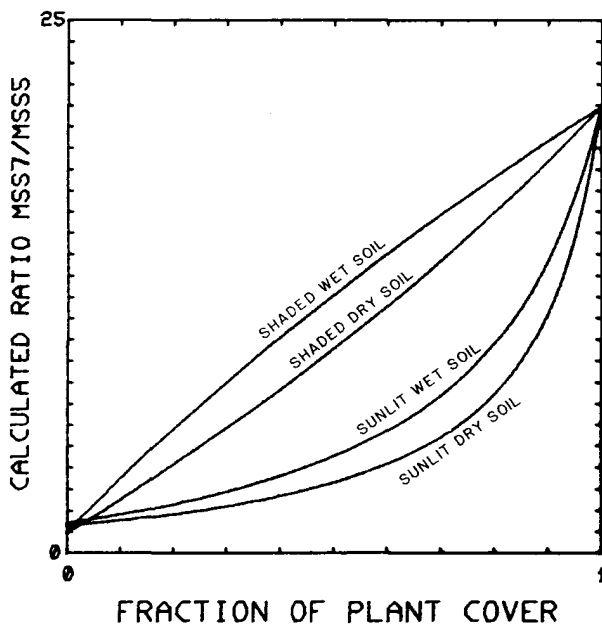


Figure 27.--Calculated IR/red ratio as a function of plant cover for the conditions of sunlit plants and sunlit and shaded, wet and dry soil.

(morning or afternoon), the ratio is nearly linearly related to plant cover. Essentially, the opposite obtains with the ND, shown in figure 28. The values for the sunlit soil conditions, representative of solar noon, are nearly linear with plant cover. For shaded conditions, the values increase rapidly for low values of plant cover and become insensitive to plant cover changes as the fraction becomes large and approaches 1. These calculations show the relative merits of the two indices with respect to sensitivity to plant cover.

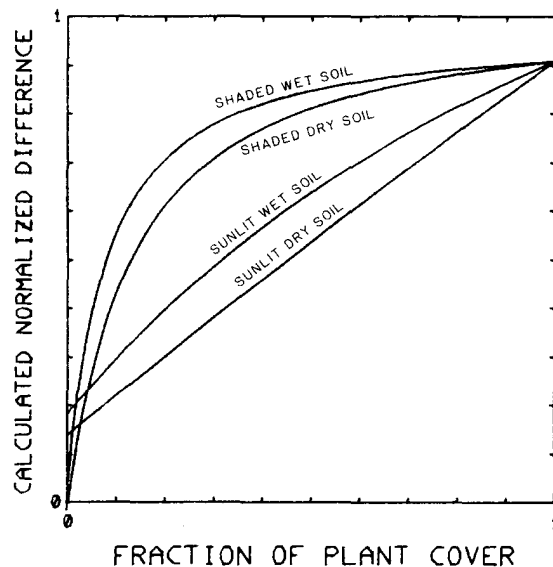


Figure 28.--Calculated normalized difference using a red (MSS5) and an infrared (MSS7) band as a function of plant cover for the conditions of sunlit plants and sunlit and shaded, wet and dry soil.

Calculations for the reflectance PVI are shown in figure 29. They show that the PVI increases linearly with plant cover. Essentially, no difference can be seen between wet and dry soil, showing the ability for the PVI to remove the soil background. The lines for shaded soil have a negative intercept. This is an indication that the soil line, extrapolated from sunlit conditions (figs. 23 and 24), is not a complete representation of the total situation and needs additional work.

## RADIOMETER RESPONSE FUNCTIONS

We have used the term "band" to signify a wavelength interval and have identified these bands with names (i.e., red, IR) and given numbers to specify the bounds (example, red band of Mark II, 0.63 to 0.69  $\mu\text{m}$ ). This implies that all of the radiation (from 0.63 to 0.69  $\mu\text{m}$ ) striking the radiometer detectors is measured. In practice, filters do not cut off radiation at precisely a given wavelength. Some radiation less than 0.63  $\mu\text{m}$  (for our example) is detected, and not all of the radiation greater than 0.63 is detected. The value of 0.63 is a nominal value. A plot of the fraction of the radiation received versus the wavelength is known as a response function. In figure 22 of the

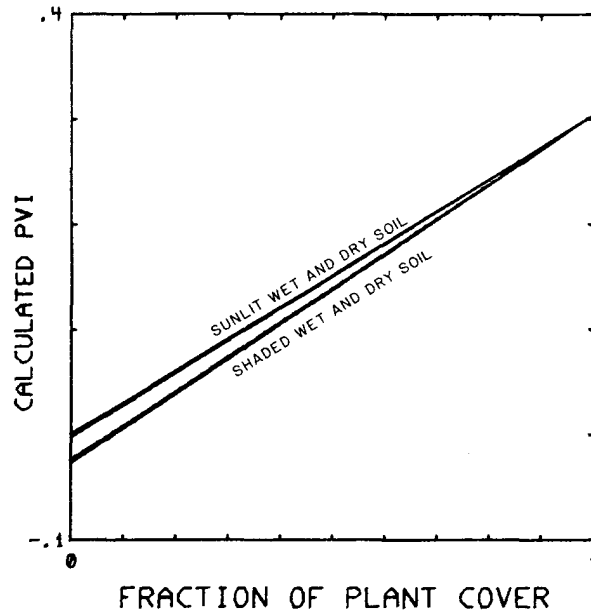


Figure 29.--Calculated Perpendicular Vegetation Index (PVI) values using MSS5 and MSS7 of the Exotech as a function of plant cover for the scene conditions, sunlit plants, sunlit wet and dry soil, and shaded wet and dry soil.

last section, spectra for soil and alfalfa were shown for the wavelength region of 0.4 to 1.0  $\mu\text{m}$ . In that figure, dashed lines were used to delineate the nominal band boundaries. Using response functions at each wavelength, the relative response can be multiplied by the spectrum for a particular target (e.g., alfalfa and soils) and summed to yield a value proportional to the actual response of a radiometer if used over the same target for which the spectrum was measured. Thus, with sets of spectra and with response functions for several instruments, different bands can be compared as to their sensitivity to vegetation, and vegetation indices can be calculated and compared among instruments.

Relative response functions for four radiometers: Relative response functions for the PMT 2-band and the Mark II 3-band are shown in figures 30 and 31. These data were provided by C. J. Tucker.<sup>4</sup> Figure 32 shows the response functions for the Exotech 4-band instrument (data provided in the instruction manual), and figure 33 presents data for the LANDSAT-1 MSS (taken from Slater 1979). The four figures have identical values for the ordinate and the abscissa to facilitate comparisons. The symbols shown in figures 32 and 33 are for the purpose of identification because of the overlapping of the bands. They are not intended to imply data points.

A comparison the PMT and the Mark II instruments shows that the red bands are nearly identical in width, whereas the IR band of the Mark II is almost twice as wide as is the IR band of the PMT. The Mark II has a band (called the water absorption band) at 1.55 to 1.75  $\mu\text{m}$  that the other three devices do not have.

<sup>4</sup>Personal communication.

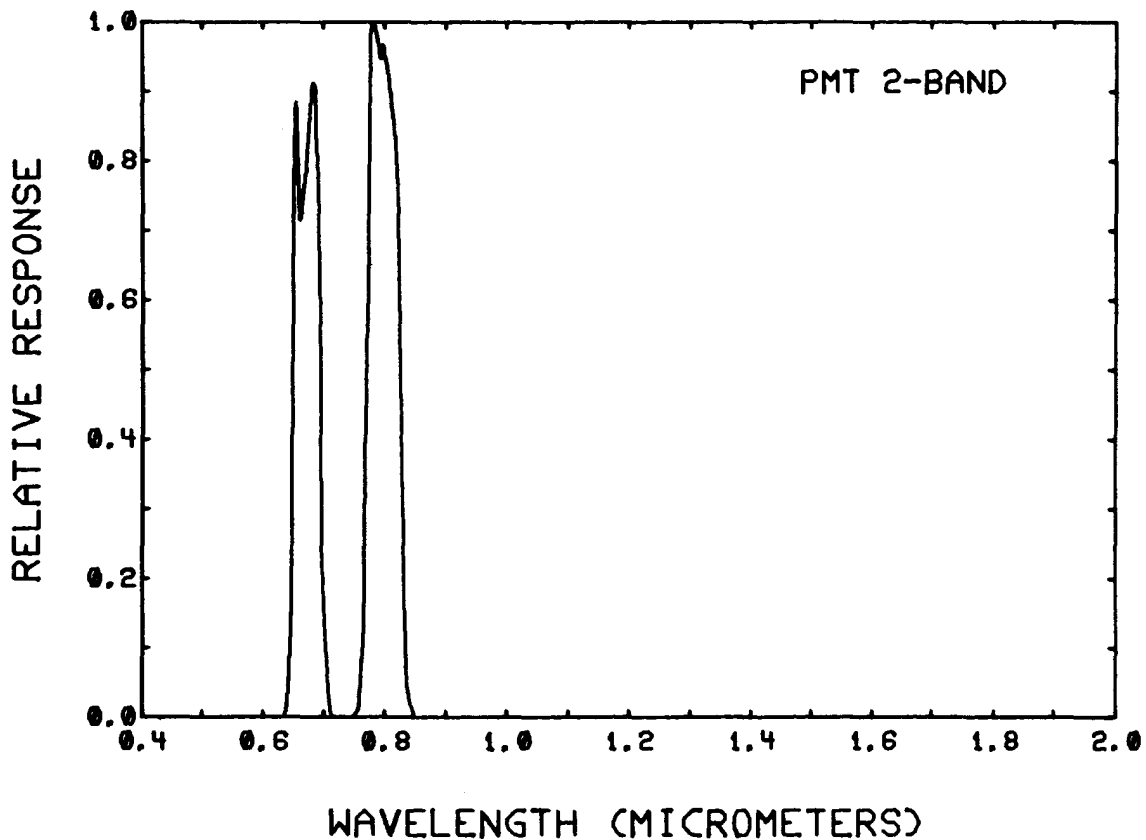


Figure 30.--Relative response functions for the PMT 2-band radiometer.

The Exotech and LANDSAT bands are much wider than any of the visible or IR bands for the PMT or the Mark II. The MSS5 band (identified with crosses in figs. 32 and 33) includes most of the area covered by the red bands of the PMT and Mark II, but is wider toward the lower wavelengths. The IR bands of the PMT and Mark II are partially included in MSS6 and are almost completely included in MSS7.

A comparison of the Exotech and the LANDSAT response functions shows that MSS4, MSS5, and MSS6 are reasonably similar, but MSS7 differs in that the Exotech appears to have about a 0.05- $\mu\text{m}$  shift towards the shorter wavelengths. The significance (or nonsignificance) of the different band widths becomes evident when relative response to spectra is calculated.

Field spectrometer data: In early April 1979, a team from NASA/GSFC<sup>5</sup> brought a field spectrometer to Phoenix to gather spectra over wheat plots at the U.S. Water Conservation Laboratory. Measurements were made over three plots, each plot containing four subplots. The three plots had been planted at different time intervals (Nov., Dec., Feb.), and the subplots received different irrigation treatments. Spectra for 2 of the 12 subplots are shown in figures 34 and 35. In figure 34, the data are for a well-watered plot planted in

---

<sup>5</sup>E. Chappelle headed the team and provided the spectrometer data.

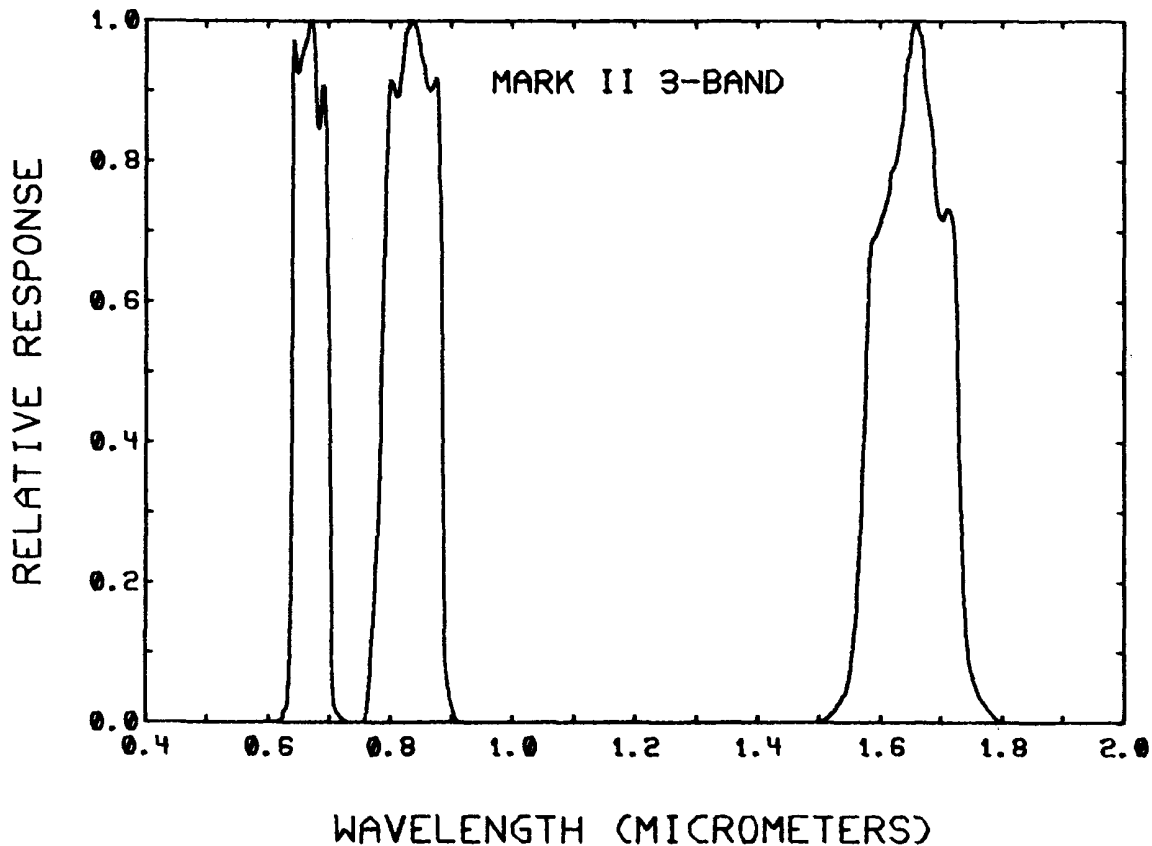


Figure 31.--Relative response functions for the Mark II 3-band radiometer.

December 1978. The plants had just begun heading and covered about 95 percent of the soil. The plants were mostly green with only a very few brown leaves showing. Figure 35 shows spectra for a plot planted in February 1979. At the time of measurement, the plants had not yet headed and covered about 40 percent of the soil. In addition to late planting, this plot received fewer than the optimum number of irrigations.

Digitized spectrometer data were interpolated to yield values at every nanometer (1/1000 of a micrometer). Response functions were digitized at each nanometer, and the product of the response function and the spectra at each nanometer within a band width was formed and summed to yield a spectral response value for each waveband on each of the four radiometers for spectra from the 12 wheat subplots. The absolute value of the summation is not of interest, but the relative magnitudes among bands and instruments allow a comparison to be made of the various bands.

The digital count range for MSS4, MSS5, and MSS6 on LANDSAT is 0 to 127. For MSS7, the range is 0 to 63. To make our results somewhat comparable to LANDSAT, we divided the summed values of response times spectra by two. We will not consider atmospheric effects on radiative transmission to satellite altitudes in this discussion. Atmospheric effects have been treated by Turner et al. (1971), Turner and Spencer (1972), and Richardson et al. (1980).

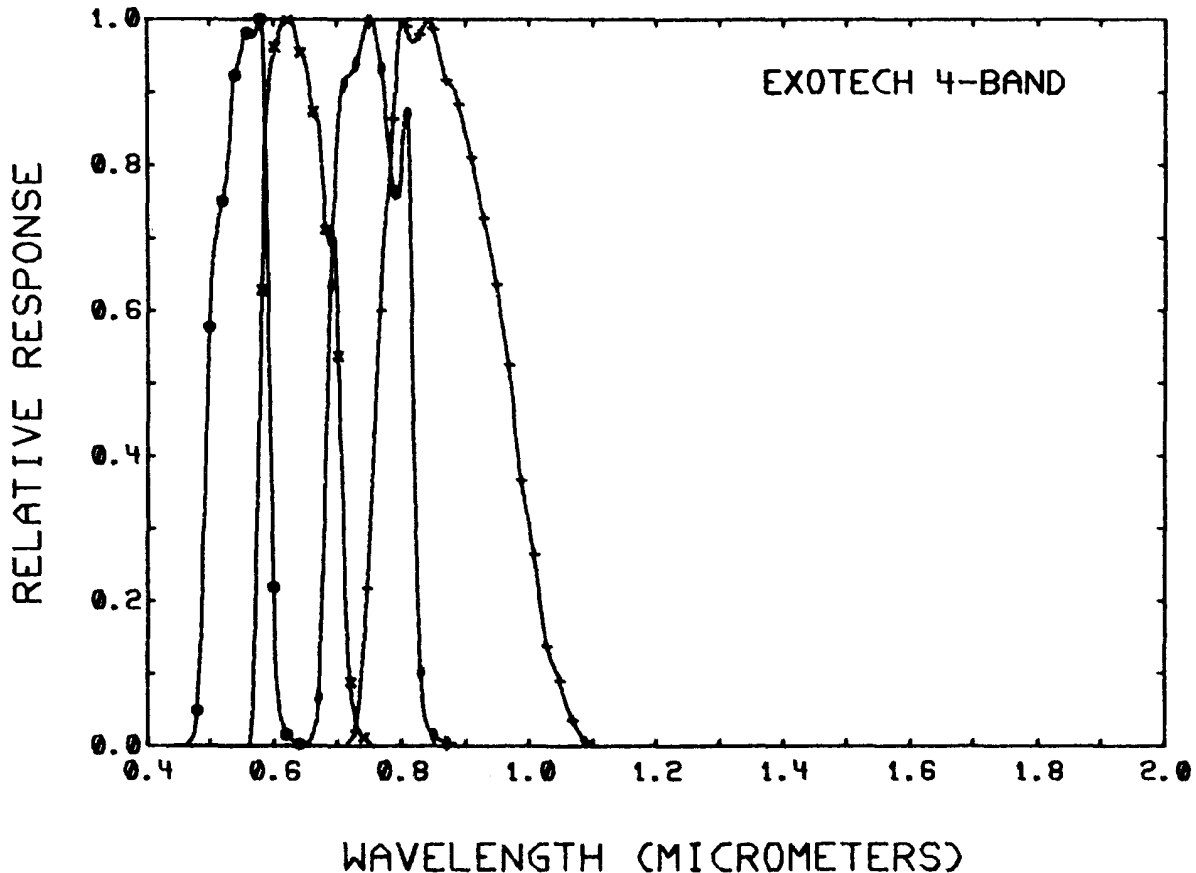


Figure 32.--Relative response functions for the Exotech 4-band radiometer. The symbols are for band identification purposes and do not imply data points.

Comparison of bands among instruments: We chose the Mark II instrument to compare with the other three radiometers in the following figures. A high correlation coefficient indicates that one instrument has no advantage over the other for obtaining information about vegetation conditions. A low coefficient indicates that one band may contain information not shown by the other.

Figure 36 compares the red band of the Mark II with the red band of the PMT 2-band instrument. As one would expect from the close alignment of the response functions (figs. 30 and 31), the correlation between the two instruments is very good, with an  $r^2 = 0.999$ . The red band of Mark II is compared with the MSS4 and MSS5 of the Exotech in figure 37. A relatively high correlation exists between the bands, especially with MSS5, which includes the red region. Similar good correlations exist between the Mark II and the LANDSAT MSS4 and MSS5 as shown in figure 38.

Figures 39, 40, and 41 compare the Mark II IR band with the PMT 2-band IR and the Exotech and LANDSAT MSS6 and MSS7 bands. Although some difference in band widths was noted for the PMT and Mark II, the IR bands are correlated with a coefficient of 0.996, indicating that the band width is not too critical if it is at a longer wavelength than about 0.75  $\mu\text{m}$  (fig. 34). This statement gains

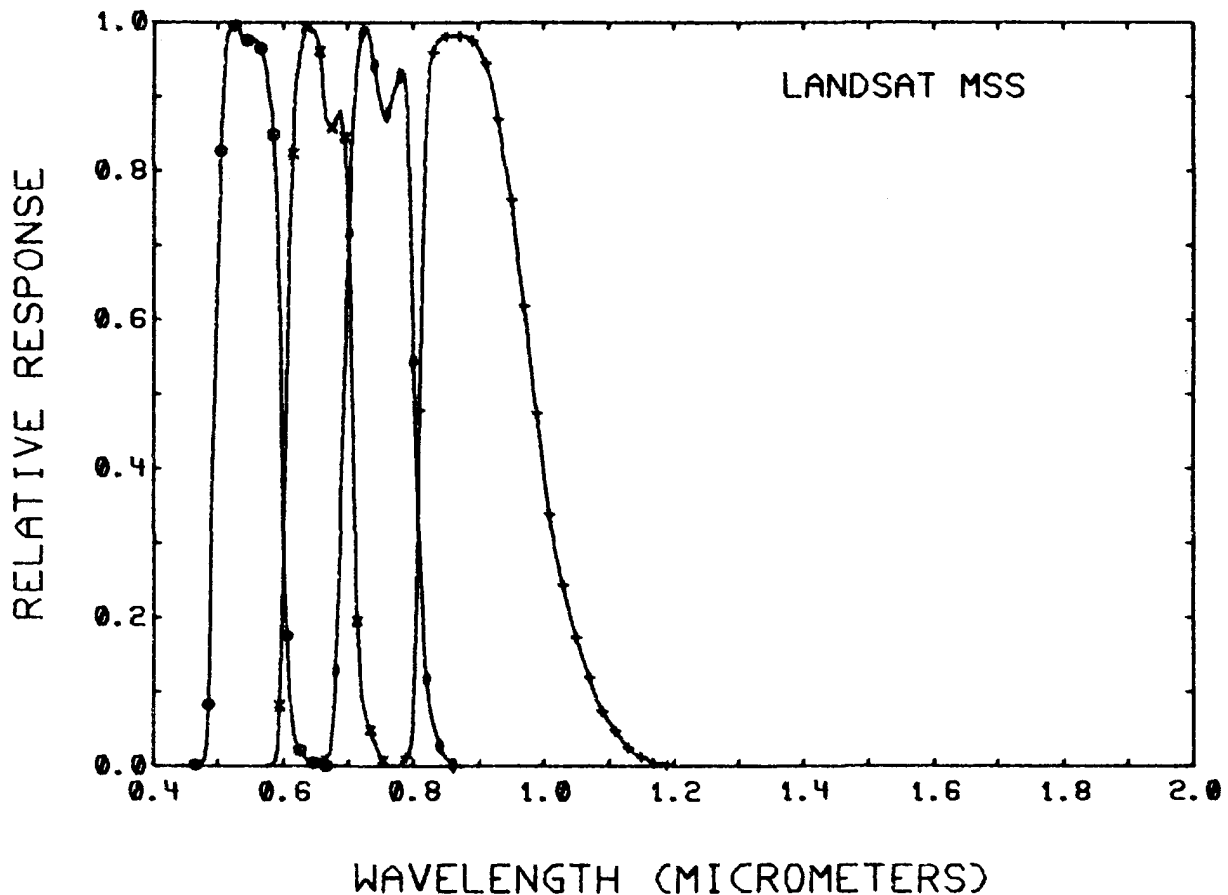


Figure 33.--Relative response functions for the LANDSAT-1 multispectral scanner. The symbols are for band identification purposes and do not imply data points.

additional support from data in figures 40 and 41 where the Exotech and LANDSAT MSS7 bands are related to the Mark II IR band with a correlation coefficient of 0.995 and 0.991, respectively. MSS6, which encompasses the abrupt shift from low to high reflectance over vegetation, shows much less correlation, having coefficients of 0.768 and 0.753.

We conclude, from the above discussion, that the red bands of the Mark II and PMT 2-band and the MSS5 of the Exotech and LANDSAT will yield equally good results over a wheat crop. Also, the Mark II and PMT IR bands and MSS7 of the Exotech and LANDSAT will give equally good results.

The water absorption band of the Mark II instrument has no comparable bands on the other three instruments. Figure 42 shows that it is not correlated with the IR band, but, as shown in figure 43, it is reasonably well correlated with the red band. Correlations ( $r^2$ ) made between all pairs of the 13 bands on the four instruments are presented in table 3. The data show that the water absorption band is reasonably well correlated with the MSS4 bands on the Exotech and LANDSAT (0.935 and 0.934), and slightly less well correlated with the MSS5 bands (0.92). The red bands on the PMT and the Mark II have coefficients of 0.896 and

Table 3.--Correlation coefficients ( $r^2$ ) between pairs of the 13 bands on 4 radiometers. Data are from applying response functions to spectra taken over 12 wheat subplots

	Exotech				LANDSAT				PMT		Mark II		
	MSS4	MSS5	MSS6	MSS7	MSS4	MSS5	MSS6	MSS7	Red	IR	Red	IR	H2O
Exotech:													
MSS4	1.0												
MSS5	.985	1.0											
MSS6	.066	.026	1.0										
MSS7	.034	.074	.805	1.0									
LANDSAT:													
MSS4	.999	.985	.063	.036	1.0								
MSS5	.983	.999	.026	.074	.984	1.0							
MSS6	.074	.031	.999	.719	.071	.031	1.0						
MSS7	.035	.074	.796	.998	.037	.075	.782	1.0					
PMT:													
Red	.967	.996	.012	.102	.969	.996	.016	.102	1.0				
IR	.037	.08	.801	.992	.039	.081	.787	.984	.108	1.0			
Mark II:													
Red	.97	.997	.014	.097	.972	.997	.017	.098	.999	.104	1.0		
IR	.035	.101	.768	.995	.055	.102	.753	.991	.132	.996	.127	1.0	
H2O	.935	.921	.109	.010	.934	.92	.118	.010	.896	.012	.901	.022	1.0

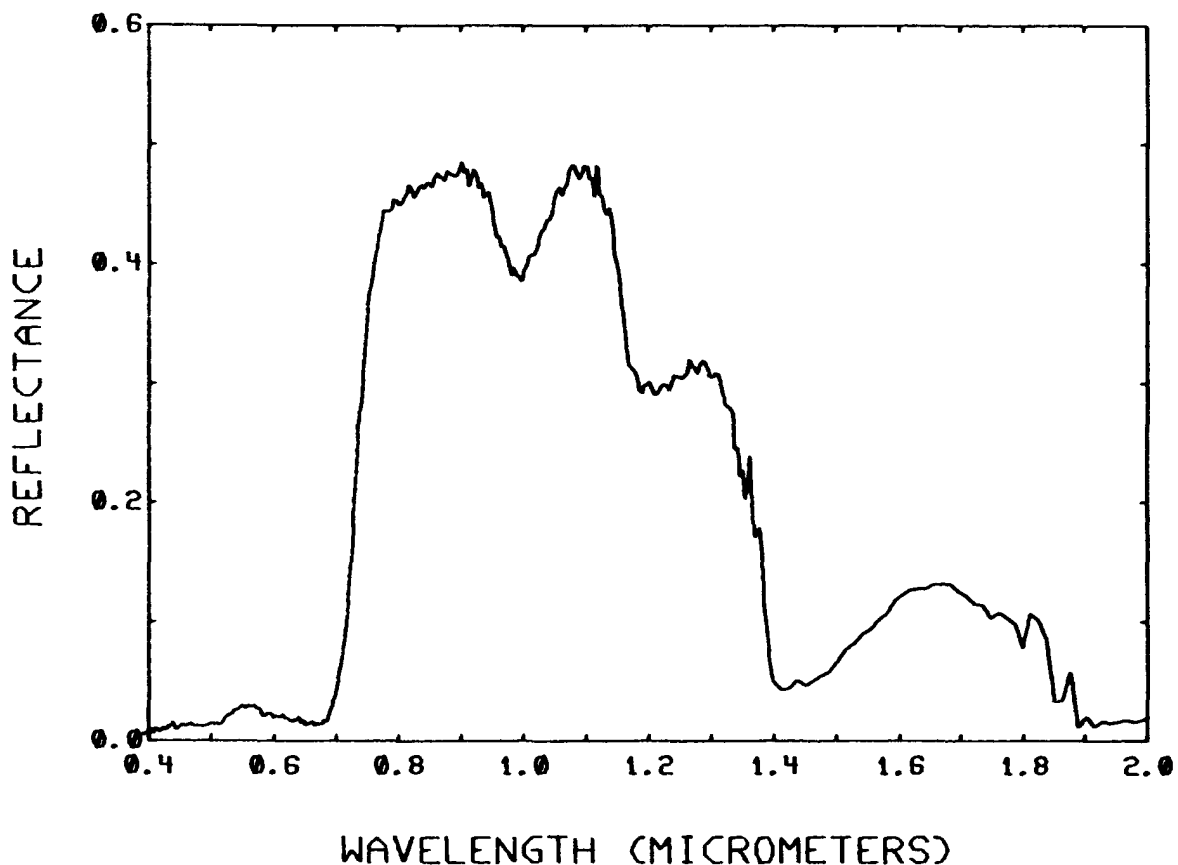


Figure 34.--Spectrum obtained over a well-watered wheat plot planted in December 1978 at Phoenix (data furnished by E. Chappelle, NASA/GSFC). Plant cover was about 95 percent.

0.901, respectively. These correlations raise the question: How much additional information is contained in the water absorption band that is not in the visible green and red bands? We pose this only as a question since we are working with a limited data set. Extensive field use of the Mark II should show the value of this band.

Comparison of vegetation indices among instruments: In addition to comparing individual bands, it is of interest to compare vegetation indices as would be obtained over the same target with different instruments. The IR/red ratios for the Mark II and the MSS7/MSS5 ratios (also IR/red but wider band widths) for the Exotech were calculated and plotted in figure 44. Linear regression analyses indicate the two ratios are linearly related with a correlation coefficient of 0.996. We conclude that over a range of vegetation densities, from about 40 percent to 100 percent cover, the ratio data from the two instruments could be readily compared using a linear transformation; however, for sparse vegetation and bare soils the data may not fit the linear function given in figure 44. Clarification of the relation for sparsely covered soils awaits more experimental data.

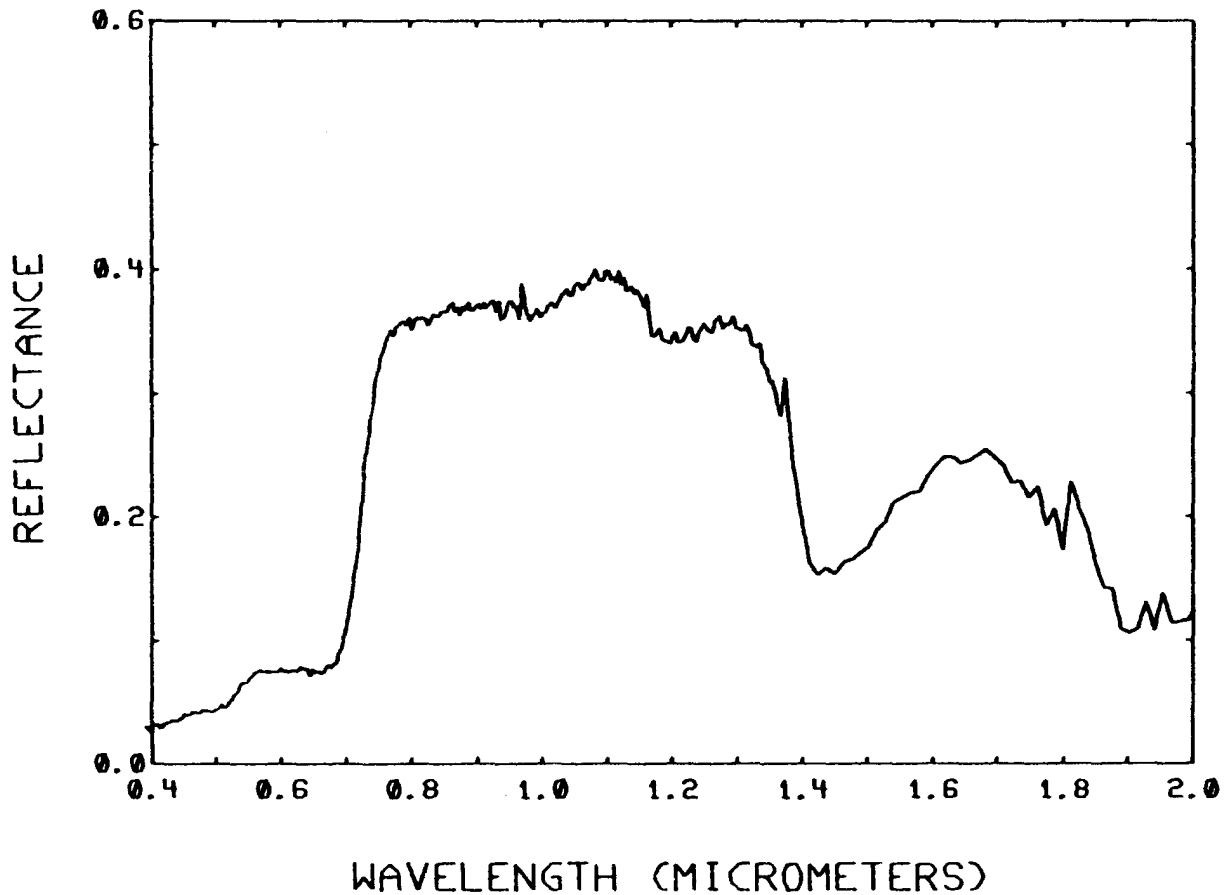


Figure 35.--Spectrum obtained over a water stressed wheat plot planted in February 1979 at Phoenix (data furnished by E. Chappelle, NASA/CSFC). Plant cover was about 40 percent.

The ND's for the two instruments are shown in figure 45. Over the range of plant densities shown here, the relationship is linear with an  $r^2$  value of 0.999; however, the nonzero intercept indicates that the relation may not be linear over the entire range from 0 percent to 100 percent plant cover.

The water absorption band: The water absorption band is sensitive to water in plants and exhibits the greatest contrast between green vegetation and bare soil (Learner et al. 1978). This sensitivity to water could greatly improve our ability to detect the presence of water stress and other factors that inhibit water uptake by plants. With a number of radiometers in this band, data should soon be available to evaluate its potential. Some questions to be answered are: Should this band be ratioed with another? If so, which one? What form of vegetation indices can enhance information in this band? Must we use reflectances or can radiances be readily corrected for sun angle?

Answers to the above and other questions await data from field experiments. The information gained by hand-held radiometers should prove to be a valuable guide to the interpretation of Thematic Mapper data that should be available after the launch of LANDSAT D.

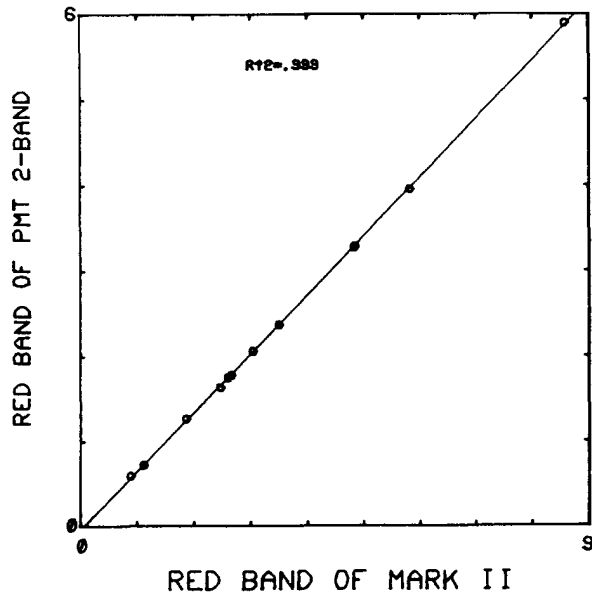


Figure 36.--A comparison of the red bands on the Mark II and the PMT 2-band. Data are for 12 wheat subplots.

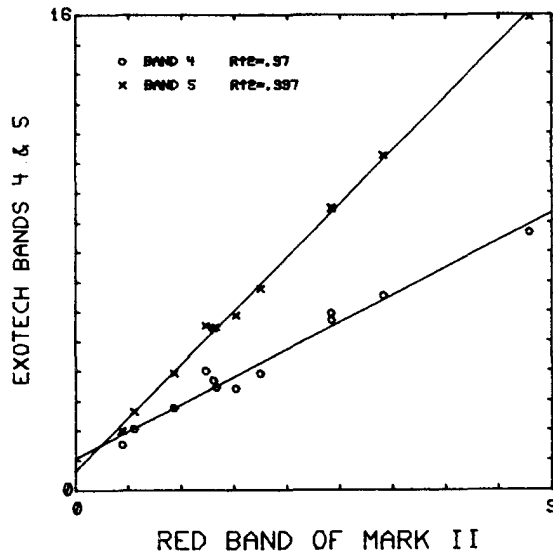


Figure 37.--A comparison of the red bands on the Mark II with MSS4 and MSS5 of the Exotech. Data are for 12 wheat subplots.

#### CALCULATION OF APPROXIMATE LOCAL STANDARD TIME FOR LANDSAT OVERPASSES

LANDSAT satellites were launched in sun synchronous orbits inclined  $99^\circ$  from the Equator, causing the satellites to cross the United States in a south-southwestwardly direction, crossing the Equator nominally at 0930 local civil time in descending mode. Precise knowledge of the local standard time that the

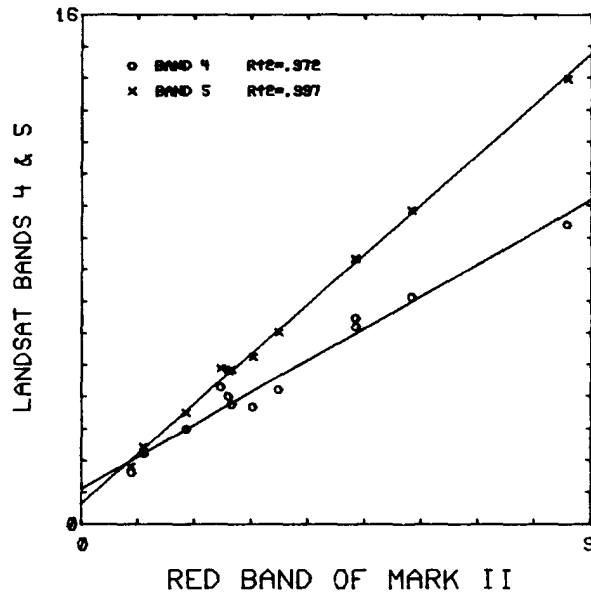


Figure 38.--A comparison of the red bands on the Mark II with MSS4 and MSS5 of LANDSAT-1. Data are for 12 wheat subplots.

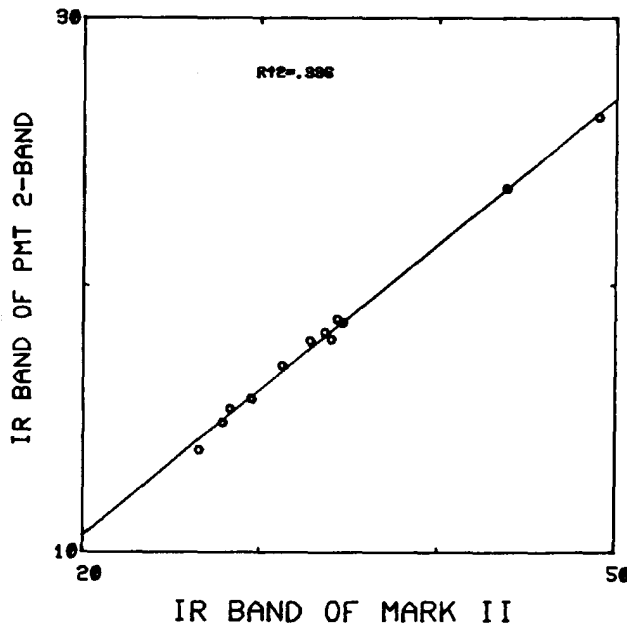


Figure 39 .--A comparison of the IR band on the Mark II with the IR band on the PMT 2-band. Data are for 12 wheat plots.

satellite will overfly particular sites in the United States is important for planning experiments in which aircraft and ground data are to be a simultaneously obtained. Duggin (1977) and Jackson et al. (1979) have shown that spectral data taken over row crops are affected by the solar elevation, and hence time of day, necessitating coincident times for satellite-aircraft and ground data collection to minimize discrepancies caused by solar elevation changes.

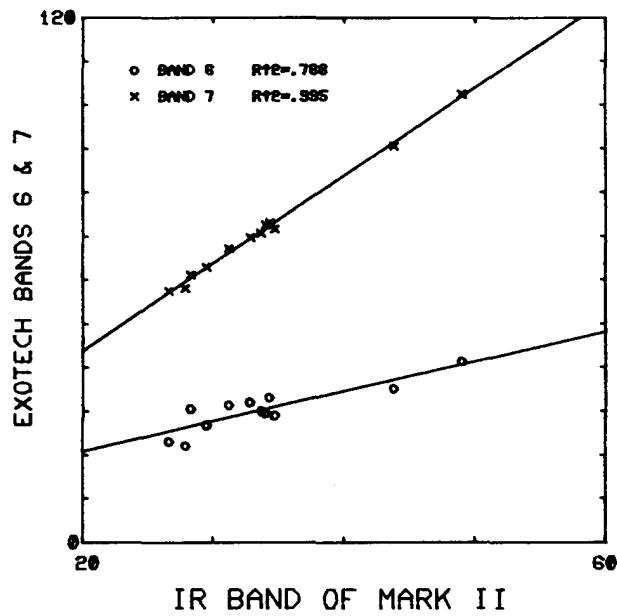


Figure 40.--Correlation of the IR band of the Mark II with MSS6 and MSS7 of the Exotech. Data are for 12 wheat subplots.

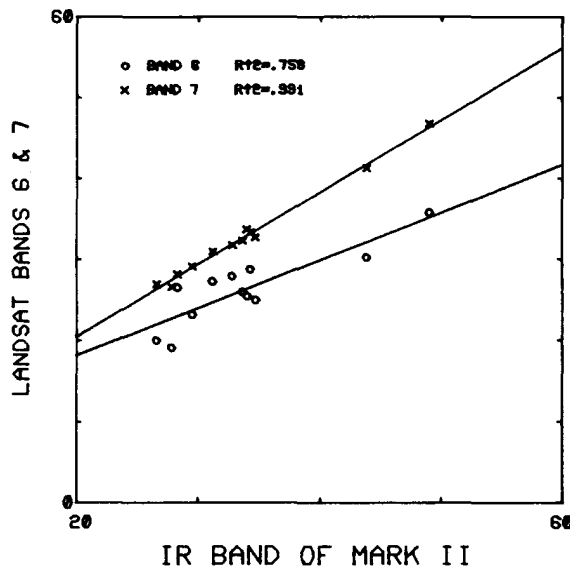


Figure 41.--A comparison of the IR band of the Mark II with MSS6 and MSS7 of LANDSAT-1. Data are for 12 wheat subplots.

Time: Time is calculated from the Greenwich meridian (zero longitude). There are three commonly used ways of reporting time: standard time, civil time, and solar time. A civil day is defined as precisely 24 hours. Thus, for each degree of longitude, the time change is  $1440 \text{ min}/360^\circ = 4 \text{ min/degree}$ . For any particular west longitude, the local civil time (LCT) is less than Greenwich time by 4 min/degree.

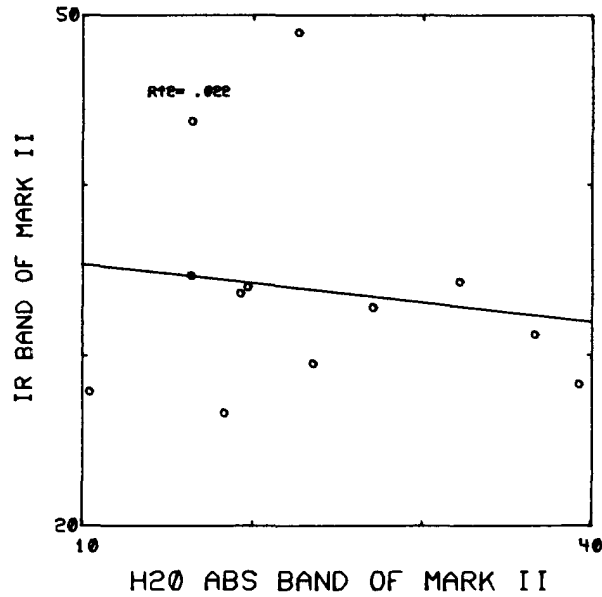


Figure 42.--A comparison of the water absorption and the IR bands of the Mark II. Data are for 12 wheat subplots.

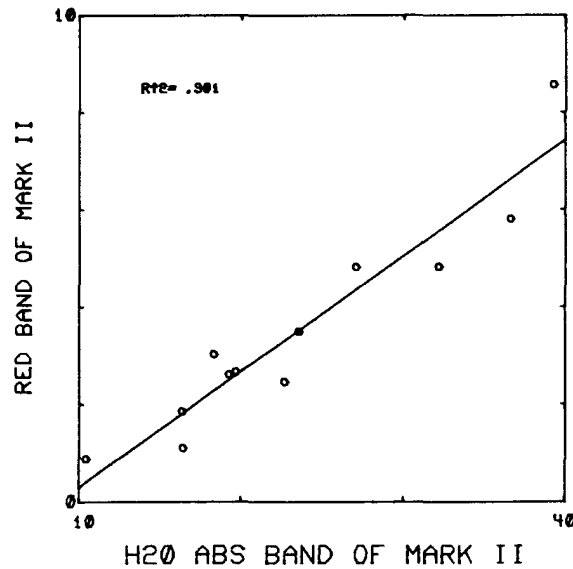


Figure 43.--A comparison of the water absorption and the red bands of the Mark II. Data are for 12 wheat subplots.

The inconvenience of using LCT for everyday use is readily apparent when one considers that every location in east-west directions has a different time. Thus, time zones have been defined with the LCT of a designated meridian near the center of the zone used for the entire zone. For the United States, these meridians are 75° W. longitude (Eastern standard time), 90° W. longitude (Central standard time), 105° W. longitude (Mountain standard time), and 120° W. longitude (Pacific standard time). Note that the difference between the meridians is 15° longitude or one hour of civil time.

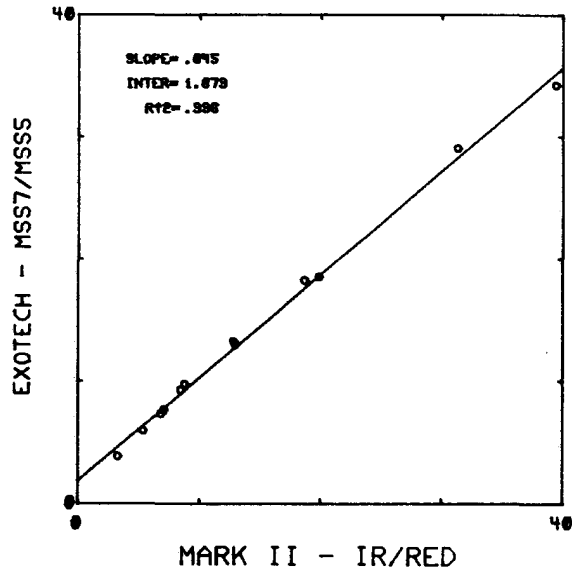
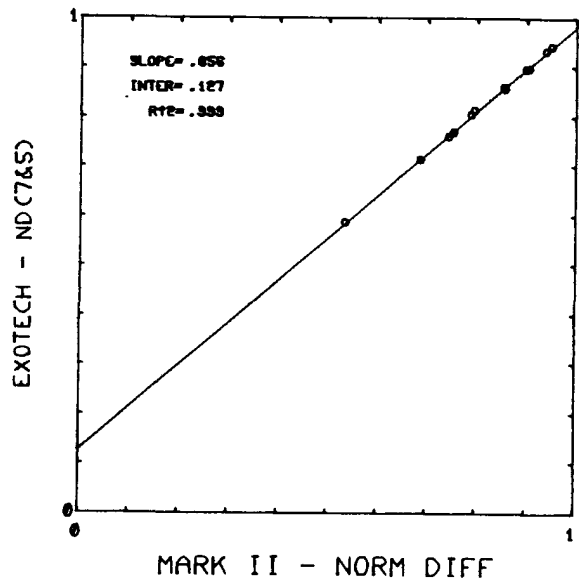


Figure 44.--A comparison of the IR/red ratios for the Mark II and the Exotech for plant cover ranging from 40 to 100 percent.

Figure 45.--A comparison of the normalized differences for the Exotech MSS5 and



MSS7 bands and the Mark II IR and red bands for plant cover ranging from 40 to 100 percent.

At a particular longitude (x), the difference between the LCT and the local standard time is:

$$\Delta T (\text{longitude}) = 4(\text{longitude of standard meridian in time zone C } x) \quad (33)$$

and the LCT at X is

$$LCT(X) = LCT(M) + \Delta T \quad (34)$$

where M designates the standard meridian within the time zone, and LCT(M) represents the standard time for that time zone.

For example, Phoenix is at about 112° W.

$$\begin{aligned} \text{LCT(Phoenix)} &= \text{LCT}(105^\circ \text{ W.}) + 4(105 - 112) && (35) \\ &= \text{LCT}(105^\circ \text{ W.}) - 28 \text{ min} \end{aligned}$$

Since LCT(105° W.) is Mountain standard time (MST), it is 1132 MST in Phoenix when it is civil noon at 105° W. Conversely, civil noon at Phoenix occurs at 1228 hours.

Solar time, the time shown by a sundial, differs from civil time by the equation of time (Threlkeld 1962). This difference is caused by irregularities in the earth's rotation, obliquity of the earth's orbit, and other factors. Values for the equation of time are given in table 4. These data, interpolated from table 14.2 of Threlkeld (1962), are for 1958. Threlkeld stated that, for practical purposes, these values could be used for any year, and that for any one day the equation of time may be considered constant. Leap year causes only a small error. From table 4, the equation of time for 15 February is about minus 14 min and for 1 November about plus 16 min. The value in table 4, for a particular day, added algebraically to LCT at the longitude of interested yields solar time. Thus, solar time at Phoenix is LCT at 105° W. minus 28 plus equation of time, and conversely, the LCT at a particular solar time is solar time plus 28 minus equation of time. As an example, solar noon at Phoenix on 15 February and 1 November would be: 1200 + 28 + 14 = 1242, and 1200 + 28 - 16 = 1212 MST, respectively.

LANDSAT overpass times: The usual response to a query as to when LANDSAT passes over is 0930. This is the nominal time that LANDSAT crosses the Equator and is given in terms of LCT. Some literature may refer to the LCT as the local mean time. If the orbits were perfectly sun synchronous, the equatorial crossing time (ECT) would be constant at near the nominal 0930; however, the three LANDSAT satellites have been slightly nonsun synchronous, and the ECT's have changed over the years (fig. 46). The ECT for LANDSAT-1 changed about 1 hour and 45 min during 6 years of operation. LANDSAT-2 underwent an orbit adjust during the period 2 November 1977 to 2 February 1978. LANDSAT-3 appears to be closest to a sun synchronous orbit of the three satellites.

The ECT versus time path can be closely approximated with a quadratic equation. For LANDSAT-3, the equation is

$$\text{ECT} = 9.47558 + 3.62836 \times 10^{-4} T - 5.20891 \times 10^{-7} T^2 \quad (36)$$

where T is the time in consecutive days since 1 January 1978. Equation 36 will approximate the ECT for LANDSAT-3 only until orbital adjustments are made. Data are periodically available from the GSFC. If extensive experiments are planned in which accurate LANDSAT crossover times are needed, consult with NASA.

Since the satellites cross the United States in a south-southwesterly direction, the orbital paths will cross a specific U.S. location at LCT some minutes ahead of the local civil ECT. The orbital path will cross several degrees of longitude in traveling from a point over the United States to a point over

Table 4.--Daily (Julian Day) values for the equation of time (EQTM in minutes) interpolated from a table given by Threlkeld (1962)

DAY	EQTM								
1	3.3	74	9.2	147	3.1	220	5.7	293	15.0
2	3.7	75	9.0	148	2.9	221	5.5	294	15.2
3	4.2	76	8.7	149	2.8	222	5.4	295	15.3
4	4.7	77	8.4	150	2.7	223	5.3	296	15.5
5	5.1	78	8.1	151	2.6	224	5.1	297	15.6
6	5.6	79	7.8	152	2.4	225	4.9	298	15.8
7	6.0	80	7.5	153	2.3	226	4.8	299	15.9
8	6.4	81	7.2	154	2.1	227	4.6	300	16.0
9	6.9	82	6.9	155	2.0	228	4.4	301	16.1
10	7.3	83	6.6	156	1.8	229	4.2	302	16.2
11	7.7	84	6.3	157	1.6	230	4.0	303	16.2
12	8.1	85	6.0	158	1.4	231	3.8	304	16.3
13	8.5	86	5.7	159	1.2	232	3.5	305	16.3
14	8.8	87	5.4	160	1.1	233	3.3	306	16.4
15	9.2	88	5.1	161	0.9	234	3.1	307	16.4
16	9.6	89	4.8	162	0.7	235	2.8	308	16.4
17	9.9	90	4.5	163	0.5	236	2.6	309	16.4
18	10.2	91	4.2	164	0.3	237	2.3	310	16.4
19	10.6	92	3.9	165	0.1	238	2.0	311	16.3
20	10.9	93	3.6	166	-	239	1.7	312	16.3
21	11.2	94	3.3	167	-	240	1.5	313	16.2
22	11.4	95	3.0	168	-	241	1.2	314	16.1
23	11.7	96	2.7	169	-	242	0.8	315	16.0
24	12.0	97	2.4	170	-	243	0.6	316	15.9
25	12.2	98	2.1	171	-	244	0.2	317	15.8
26	12.5	99	1.8	172	-	245	0.1	318	15.6
27	12.7	100	1.6	173	-	246	0.4	319	15.5
28	12.9	101	1.3	174	-	247	0.7	320	15.3
29	13.1	102	1.0	175	-	248	1.0	321	15.1
30	13.2	103	0.8	176	-	249	1.4	322	14.9
31	13.4	104	0.5	177	-	250	1.7	323	14.7
32	13.6	105	0.3	178	-	251	2.0	324	14.5
33	13.7	106	0.0	179	-	252	2.4	325	14.3
34	13.8	107	0.2	180	-	253	2.7	326	14.0
35	14.0	108	0.5	181	-	254	3.1	327	13.8
36	14.1	109	0.7	182	-	255	3.4	328	13.5
37	14.1	110	0.9	183	-	256	3.8	329	13.2
38	14.2	111	1.1	184	-	257	4.1	330	12.9
39	14.2	112	1.3	185	-	258	4.5	331	12.6
40	14.3	113	1.5	186	-	259	4.8	332	12.3
41	14.3	114	1.7	187	-	260	5.2	333	11.9
42	14.3	115	1.9	188	-	261	5.5	334	11.6
43	14.3	116	2.1	189	-	262	5.9	335	11.2
44	14.3	117	2.2	190	-	263	6.3	336	10.9
45	14.3	118	2.4	191	-	264	6.6	337	10.5
46	14.3	119	2.5	192	-	265	7.0	338	10.1
47	14.2	120	2.7	193	-	266	7.3	339	9.7
48	14.1	121	2.8	194	-	267	7.7	340	9.3
49	14.1	122	3.0	195	-	268	8.0	341	8.9
50	14.0	123	3.1	196	-	269	8.4	342	8.4
51	13.9	124	3.2	197	-	270	8.7	343	8.0
52	13.8	125	3.3	198	-	271	9.0	344	7.5
53	13.7	126	3.4	199	-	272	9.4	345	7.1
54	13.6	127	3.4	200	-	273	9.7	346	6.6
55	13.4	128	3.5	201	-	274	10.0	347	6.2
56	13.3	129	3.6	202	-	275	10.4	348	5.7
57	13.1	130	3.6	203	-	276	10.7	349	5.2
58	13.0	131	3.7	204	-	277	11.0	350	4.8
59	12.8	132	3.7	205	-	278	11.3	351	4.3
60	12.6	133	3.7	206	-	279	11.6	352	3.8
61	12.4	134	3.7	207	-	280	11.9	353	3.3
62	12.2	135	3.7	208	-	281	12.2	354	2.8
63	12.0	136	3.7	209	-	282	12.5	355	2.3
64	11.8	137	3.7	210	-	283	12.7	356	1.8
65	11.6	138	3.7	211	-	284	13.0	357	1.3
66	11.3	139	3.7	212	-	285	13.3	358	0.7
67	11.1	140	3.6	213	-	286	13.5	359	0.2
68	10.8	141	3.6	214	-	287	13.8	360	0.3
69	10.6	142	3.5	215	-	288	14.0	361	0.8
70	10.3	143	3.4	216	-	289	14.2	362	1.3
71	10.0	144	3.3	217	-	290	14.4	363	1.8
72	9.8	145	3.3	218	-	291	14.6	364	2.3
73	9.5	146	3.2	219	-	292	14.8	365	2.8

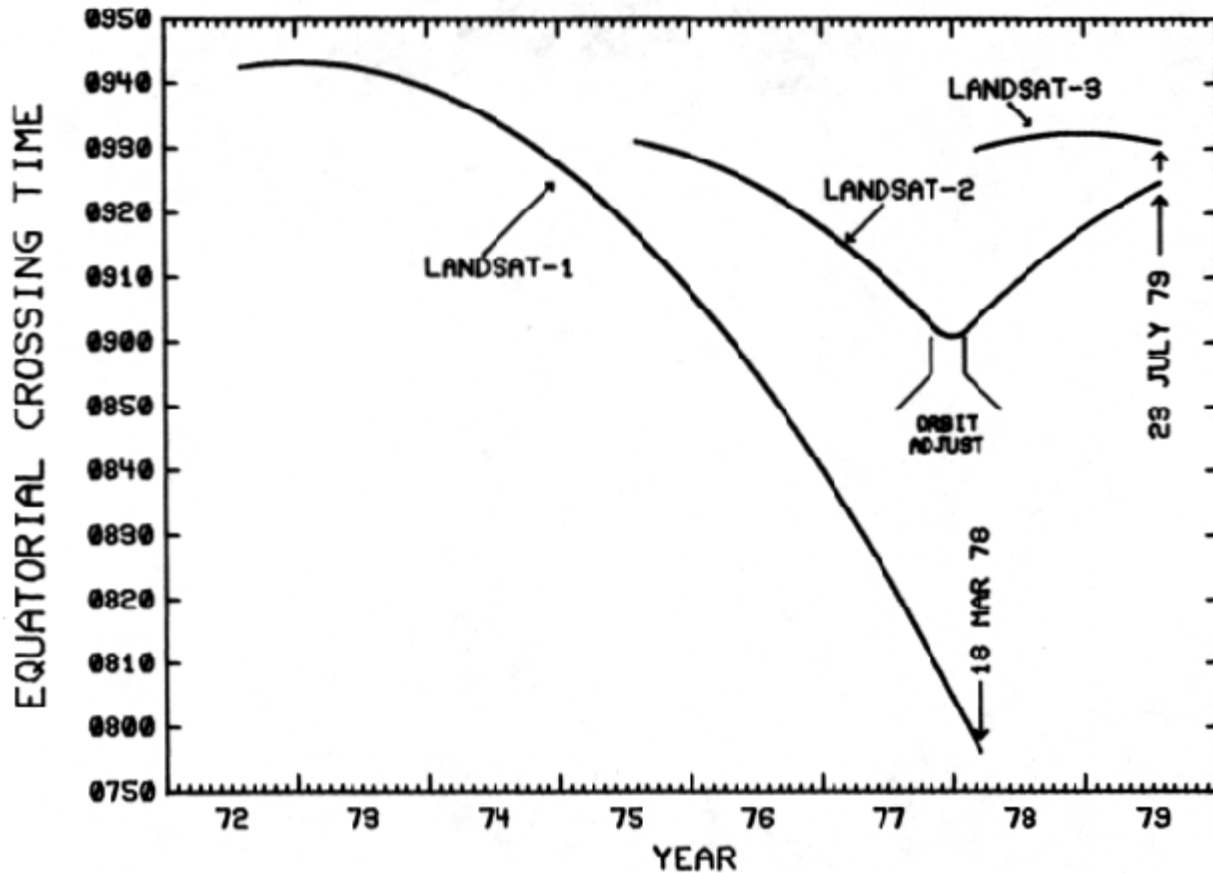


Figure 46.--Equatorial crossing time (local civil or mean time) for the three LANDSAT satellites. The last data shown are for 23 July 1979. (Data furnished by John Price, NASA/GSFC).

the Equator. The exact number of degrees displacement depends upon the latitudinal distance of the ground site of interest from the equator. Figure 47 shows the time difference that adjusts the ECT to a particular latitude in the northern hemisphere. These data account for the longitudinal change. For Phoenix (33°26' N., 112°01' W.), the time difference is about 21 min, assuming that the orbital path is directly above Phoenix. An approximate equation for this time difference is

$$\Delta T (\text{latitude}) = 0.433098 L + 6.58729 \times 10^{-3} L^2 \quad (37)$$

where  $\Delta T$  (latitude) is in minutes and  $L$  is in degrees north latitude.

To calculate the local standard time for a LANDSAT-3 overpass for a particular latitude and longitude:

- (a) Use equation 36 to estimate the ECT for the particular day.
- (b) Use equation 37 to estimate the  $\Delta T$  (latitude) adjustment (in minutes).
- (c) Calculate  $\Delta T$  (longitude) from equation 33 (in minutes).
- (d) Add (a) + (b) + (c).

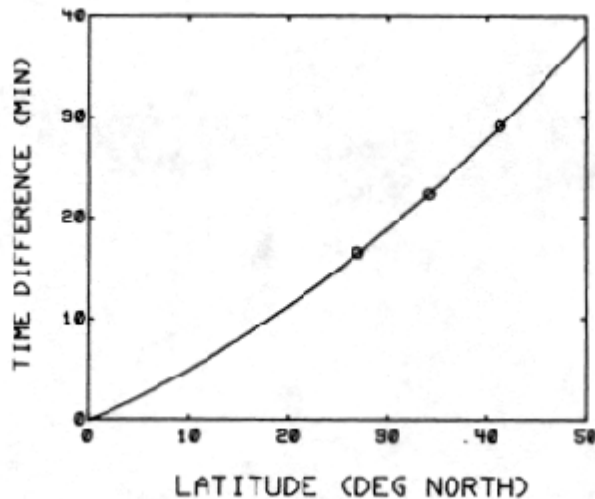


Figure 47.--The time difference in minutes between the local civil time at a particular north latitude and the local civil time of equatorial crossing (data furnished by NASA/GSFC).

Example: The LANDSAT-3 overpass time for 18 July 1979 on the nearest orbital track over Phoenix was

- (a) 18 July 1979 was day  $365 + 199 = 564$ . Using equation 36, ECT = 9.515 hours (0931).
- (b)  $\Delta T$  ( $33^\circ$  lat.) = 21.46 min (round to 21).
- (c)  $\Delta T$  ( $112^\circ$  long.) = 28 min.
- (d)  $0931 + 21 \text{ min} + 28 \text{ min} = 1020 \text{ MST}$ .

The value of 1020 will decrease slightly with time until the orbit is adjusted. If no orbital adjustments are made, on 1 January 1981, the overpass time will be at approximately 1004 MST.

LANDSAT orbit tracks are approximately  $1.43^\circ$  of longitude apart. This translates to 5.7 min. Therefore, the overpass time is bracketed by .2.9 min to allow for the fact that the satellite may not be directly overhead. Maps showing the orbit path are available from NASA. These maps also give the date of overpass. LANDSAT's repeat cycle is 18 days.

## INFRARED THERMOMETERS

IR thermometers provide a noncontact means for measuring the apparent emitted thermal radiation from an object. If the emissivity<sup>6</sup> of the object is known (the emissivity of most vegetation and soil surfaces is between 0.93 and

---

<sup>6</sup> Emissivity refers to the relative efficiency with which an object emits radiation. Swain and Davis (1978) define it as "the ratio of the radiation given off by a surface to the radiation given off by a blackbody at the same temperature; a blackbody has an emissivity of 1, other objects between 0 and 1."

0.97, for complex canopy structures it approaches 1.0), the absolute temperature can then be determined. Scanning IR thermometers mounted in aircraft and satellite platforms are able to collect data over broad regions, while portable hand-held devices can be used on the ground to provide temperatures of more limited, identified targets. Two major advantages of IR thermometers are their capability to rapidly determine temperatures remotely and nondestructively and to integrate temperatures areally over the entire field of view, thus avoiding single point measurement and the associated sampling problems.

Many types of hand-held IR thermometers are available. The February 1980 issue of "Measurements and Control" gives an extensive list of commercially available instruments, with specifications, prices, and manufacturer's addresses.

Field use: To obtain representative canopy temperatures, it is desirable to point the IR thermometer so that a maximum amount of vegetation is viewed by the sensor. This can be accomplished by viewing the target obliquely and at right angles to any structures that might be present in the field. The target area viewed by a circular field-of-view instrument when deployed in an oblique fashion is teardrop shaped, and the upper edge of the target is much higher than one might intuitively expect (especially with larger, i.e., 20°, field-of-view lenses). We usually take readings looking in several different directions to minimize effects that insolation angle and viewing azimuth angle may have on apparent target temperature. Our routine measurements are taken 1 to 2 hours following solar noon, a time when a maximum difference between canopy and air temperature usually occurs. Routine weather observations, i.e., cloud cover, windspeed, precipitation, target conditions, and wet and dry bulb air temperatures, are recorded whenever canopy temperatures are measured.

Calibrations: Experience has shown us that the readout temperature on most factory calibrated instruments is not an accurate representation of apparent blackbody temperatures. This probably results from the fact that calibration is a tedious and difficult procedure for which good standards have not yet been devised and also because the calibrations of each instrument tend to drift with age of the electronics, the sensors, and the wear and tear of field usage. For these reasons, we calibrate all instruments as precisely as possible under standardized conditions using a precision blackbody calibration device. Such calibrations are routinely carried out at 2- to 4-week intervals and whenever an instrument is suspected to be in error. Care is taken to calibrate instruments as close as possible to the manner in which they are used in the field. For example, both the PRT-5 and Telatemp are calibrated on battery rather than line power because they are rarely used in the field on line power. Since the calibrations of our IR thermometers are usually linear, it is a simple matter to arrive at corrected apparent temperatures in the field either with a portable calculator or a calibration curve, or after collecting instrument readout data, to make the corrections on a computer.

To keep constant check on thermometers between calibrations, we have found it helpful to institute a two-temperature calibration check each time the instruments are used. We suspended a black cavity into an inexpensive circulating water bath and then simultaneously recorded the temperature of the water with a mercury-in-glass thermometer and the temperature of the black cavity with the IR thermometer. A heater in the water bath was used to raise the temperature

of the water by 10° to 15°C so that about 20 min later, after canopy temperatures were taken, a second calibration check at the higher temperature could be made. Any deviation from the expected is an indication that the IR thermometer needs recalibration. Certain manufacturers will provide a black-body plate with a thermometer imbedded in it to perform these daily checks. Used in a fairly stable environment with no direct insolation falling on the plate, these will probably provide an excellent way to check the daily performance of the IR thermometer. We cannot overstress the importance of good calibration and regular daily checks.

Precautions: We have noted the following precautions in the use of IR thermometers, which we share with other users with the hope it will spare them having to discover it for themselves.

a) Temperature equilibrium and warm-up periods. Laboratory calibrations have determined that the most reliable data can be expected when the instruments have been equilibrated out-of-doors in the shade for about 30 min prior to the readings. This allows the electronics and the housing of the instrument to come to equilibrium with the air temperature and generally gives more stable readings. In addition, the air-temperature sensor provided on the AG-42 will not give correct target-air differentials unless this procedure is followed. Taking the IR thermometer out of a air-conditioned pickup and immediately using it in 110°F air temperatures is not suggested when target-air differentials are required. Also, the target-air differential must be calibrated in a known temperature room before the data in that mode can be trusted, because the factory calibration of the thermistor air temperature device may be in error. The PRT-5 requires an initial warmup so that the internal reference temperature will heat up sufficiently and stabilize. The AG-42 does not require "on" time to warm up. The instrument "comes to life" instantly upon demand.

b) Operation in a "noisy" environment. Instruments should not be calibrated or operated in any area that might be considered noisy from an electrical signal standpoint. We have found that stray signals from electronic devices and CB radios can change the output of some instruments.

c) Operation in dusty environment. This should be avoided when possible. Dust should not be allowed to accumulate on the optics of the instruments. It can be removed by blasts of Dust Off, a commercially available product used in the photography industry.

Caution: Do not use Dust Off prior to or during any measurements or calibrations. The refrigerant propellant 2,2-4 dichloro-difluoroethane used in that product is an effective filter in a portion of the thermal spectrum. It will alter apparent temperatures significantly, especially if the target temperature is different from air temperature. After a blast of Dust Off, we found that apparent temperature of a target was 36°C when its true temperature was 40°C and the air temperature was 25°C. We found this effect persists much longer than expected (15 to 30 min).

d) Miscellaneous precautions and procedures. Do not allow instruments to get wet or allow water to enter the lens areas. Leave the instruments on charge when they are not in use. Both the PRT-5 and Telatemp have trickle charging circuits so that the batteries cannot be overcharged. Do not point the sensor at the sun.

Due to the time constants of the AG-42, more time (~5 sec) must be given for the thermometer to reach a stable reading when targets alternate between very hot soil to cool plants than if the targets are consistently within the same temperature range.

The AG-42 has the capability of measuring not only the target surface temperature but also the target-air temperature differential. This latter parameter is obtained by merely pulling the trigger on the gun when pointing it at the surface of interest. A few precautions are in order in using this capability. The thermistor, which senses air temperatures, is housed in the front part of the gun and consequently is slightly influenced by the surrounding metal. Equilibrating the gun out-of-doors for about 30 min tends to minimize the influence of the housing on the reading of the thermistor; however, we have found in some of our laboratory tests that the thermistor may actually be reading about a degree lower than the ambient air temperature. As a consequence, a separate calibration should be made if the AG-42 is to be used in the target- air differential mode.

We have observed that it is not possible to get an accurate reading while walking with the PRT-5 due to the needle fluctuations of the analog readout.

Shade must be provided for the AG-42 digital readout. The red LED display washes out in normal daylight. Shading can be effected by slipping the leather holster or a length of 3-inch-diameter black PVC over the rear of the gun.

A helpful exercise for each operator to go through before using an IR thermometer is to determine its field of view. Mount the instrument on a tripod at about the same height and angle that would be used in the field when looking at a crop. While one person observes the readout, another person should be on one side of the estimated field of view with a small piece of aluminum foil. Place the foil on the ground and move it towards the field of view. The operator can tell from the output of the IR thermometer when the foil comes within the field of view as the temperature will drop considerably. (Aluminum has an emissivity of ~0.08.) Place a stake at this particular point tangent to the field of view. The foil mover can go around the field of view of the instrument placing stakes and can mark out fairly well the area seen by the instrument when held in the normal oblique position. The same procedure can be used if the gun is to be held looking straight down.

## **PHOTOGRAPHIC DETERMINATION OF CANOPY COVER**

An estimate of percent plant canopy cover is useful when interpreting remotely sensed measurements. It is important to know what proportion of the target area viewed by a radiometer is green canopy and how much is bare soil or senescent brown or yellow leaves. We have found that color slides taken at weekly intervals throughout the growing season are sufficient to quantify these cover relationships. The technique is inexpensive, fairly rapid, and yields reproducible results. In addition to providing a means for quantifying cover relationships in situ, photographs are invaluable for documenting the general growth patterns and vigor of the plants, determining phenological growth stages, and documenting canopy architecture, lodging, and visual symptoms of nutrient

deficiency, disease, and insect damage. In some instances, it is possible to monitor a plant's short-term response to water stress such as leaf rolling or curling--a condition that can not be easily documented by other measurement techniques.

We take two nadir-oriented and one oblique photograph per plot each week. The nadir-oriented pictures are taken looking straight down at the same target areas each time from a height of about 2 m. Photographs are normally taken at 1/60 sec using ASA 64 color slide film and focusing approximately one-third of the way into the canopy. The photographs are usually taken around solar-noon so that the depth of light penetration into the canopy is near maximum and the high light levels result in the greatest possible depth of field. We use an automatic exposure, motor-driven, 35-mm camera, equipped with a 50-mm focal length, f. 1.8 lens, which has a horizontal field-of-view of about 46°. It also has a data back, which enables each frame to be labeled with a scene identification code or the calendar date. Resultant slides are projected onto a 50C by 70-cm screen of white gridded posterboard on which 200 dots were randomly positioned. Each dot is classified according to the type of target it "hits." The grid network on the screen reduces the chances of double counting a particular dot. Tabulation is facilitated by a mechanical counter. The categories we use to classify hits are bare soil, sunlit and shaded; green leaves, sunlit and shaded; brown leaves, sunlit and shaded; heads, sunlit and shaded; awes; unclassified shadow; and comments. Examples of percent green cover, percent brown cover, and percent bare soil data are given in figure 48. The data show the type of results one might expect from wheat canopies planted at different times of the year.

There is a systematic bias introduced whenever a lens with a field-of-view greater than zero is used. Although wide-angle lenses may seem attractive because of the relatively larger target area that can be viewed, their use should be avoided. Plants at the perimeter of images taken with wide-angle lenses (i.e., focal length <50 mm) will be viewed obliquely and thus present more cross-sectional percent cover than would occur if one were to look straight down on the images. This is the same problem that exists with radio meters as was discussed in section 5. The data presented in figure 48 have not been corrected for field-of-view induced bias; however, we attempted to minimize this error by projecting the slides so that only the center two-thirds of the photograph is analyzed. Williams (1979) presented an error analysis of the photographic technique for measuring percent vegetative cover.

## **STANDARDIZATION OF MEASUREMENTS AND RECORDING OF ENVIRONMENTAL CONDITIONS**

During the American Society of Agronomy meetings at Ft. Collins, Colo. (August 1979), the yield modeling group met to develop a set of standards to strive for uniformity in data collection with hand-held radiometers. Armand Bauer collected the various comments and put together an excellent set of instructions. The following is taken directly from Bauer's letter of 13 August

1979.

1. Maintain two bare soil areas as a reference in the field in which measurements are made. One should be kept "natural" (exposed to

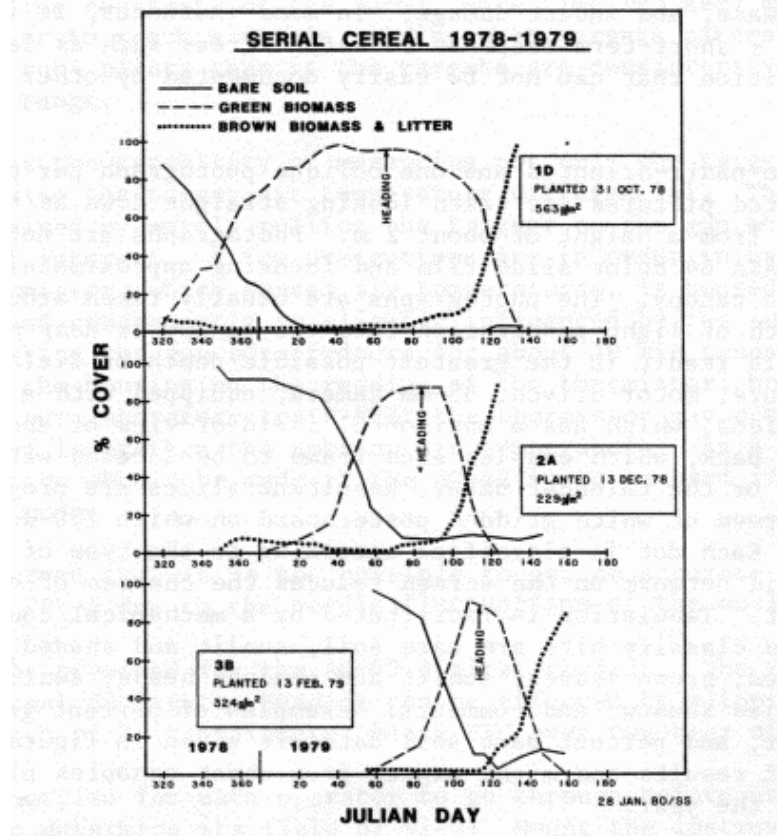


Figure 8.--Fraction of bare soil, green biomass, and brown biomass for three wheat plots over a growing season.

air) and other made wet before measurement is made. Surface should be smooth or should have the same surface roughness as the field in which measurements are made. If tillage is a variable, maintain areas of surface roughness included in the experiment.

2. Be consistent in the time of day that reflection measurements are made.

- a. Record the exact location of each site. Specify by latitude and longitude.
- b. Record time of day measurements are made (begin, end). Solar noon one hour is preferred.
- c. Daily measurements are preferred - best results usually are obtained on sunny days.
- d. Keep a log of prevailing weather conditions during time of measurement.
- e. Record the row direction.
- f. Caution
  - (1) Onset of stress, or stress affects reflectance.
  - (2) Wind increases the "error" in data.
  - (3) Avoid days with high cirrus clouds; days as free of clouds as possible are preferred.

3. Number of measurements per plot.
  - a. Depends on growth stage, but a minimum of six per plot is recommended. Don't stand in one plot to make these. Take the first one over the row (eyeballed) - take step - take reading - take step - take reading, etc.
  - b. Ray Jackson can be contacted if more detailed information is needed.
4. Height above crop that radiometer is to be held.

Recommend a minimum of one meter above top of crop canopy. Precision is greater with heights above one meter.
5. Orientation while holding instrument when measurements are made.
  - a. Whenever possible, stand to north and extend hand-held radio meter toward south.
  - b. Avoid measurements in shadows cast by reader or by other extraneous sources.
  - c. Be consistent.
6. Instrument bearer should avoid wearing light-colored clothes; avoid white shoes or bare feet.
7. BaSO<sub>4</sub> plates for calibration will be supplied with the instrument. Avoid scratching, abrasion, etc. Keep protected from elements of weather when not in use. Insects (especially grasshoppers) are "bad news" if they crawl on the plates.
8. Remember to maintain a log of "standardized" plant data. (Percent cover etc.; take pictures when possible.)
9. Keep track of everything you do. This may provide clues to improvement in use of the instrument.

## **PROCEDURES IN SUPPORT OF HAND-HELD RADIOMETER OBSERVATIONS**

At the SEA/AR Yield Group meeting in August 1979 at Ft. Collins, Colo., Craig Wiegand was asked to provide information in addition to that contained in Armand Bauer's letter (previous section). Wiegand's material is presented in this section.

### **A. Hand-held radiometer measurements**

1. Record the time of each plot or treatment observations to the nearest 5 minutes (ideally a daily check of the National Bureau of Standards, Greenwich meridian time from radio station WWV would be helpful).
2. Soil background showing through the canopy will affect readings. Therefore, (a) remove plants from a small area (in plots or turn-row)

that are tilled the same as the area where canopy measurements are made, and make same spectral observations as over canopies, (b) note whether soil surface is visibly wet or dry at time of observations, and (c) work, if can, in fields that have been soil mapped by SCS and superimpose this information on experimental areas used, and (d) graph bare soil readings along with canopy readings as a  $f(\text{time})$ . The spectral observations for the canopy variables should extrapolate to the soil background observation at zero leaf area index, biomass or plant height if surface conditions of the soil are the same at bare soil sites as at the cropped sites.

3. The proportion of the incident sunlight that is specular versus diffuse on a given measurement day may prove to be a useful characterizer of atmospheric condition. Thus, it may prove useful to obtain radiance measurements of selected canopy sites, the reference panel, and the bare soil areas when shaded and unshaded. Shading can be accomplished by fixing a piece of plywood, sheet aluminum, or even cardboard to a pole and shading the area where measurements are made. Size of the shaded area should be such that the field of view of the hand-held radiometer is completely filled by shadow. A minimum size shade is probably about twice the size of the reflectance standard; it should be held high enough above the target that 10 percent or less of the sky is obscured.
  - a. The shadowed observations yield information on the signal expected from the shadows within the canopies. (The major components of the spectral signals are sunlit vegetation, sunlit soil, and shadowed leaves and soil.)
  - b. Note: Irradiance is a measure of hemispherical downwelling energy influx; it is usually measured with the sensor pointing upward with a cosine response diffuser over the sensor. Radiance measurements are made looking downward with an instrument that has a small solid angle field of view (say from 2 to 20 degrees) such as the hand-held radiometers have. (See attached reference on terminology.) The radiance measurement for the sunlit reference panel is proportional to the specular solar plus diffuse sky irradiance. The shaded panel reading represents the diffuse (or sky) irradiance. Subtraction of the shaded reading from the sunlit reading yields the specular irradiance component of the incident flux.

Caution: For irradiance to be inferred from radiance measurements the surfaces have to be Lambertian (perfect diffusers). The  $\text{BaSO}_4$  panel, plant leaves and soil are not perfectly Lambertian but come fairly close.

4. Although signals will be lower, bidirectional reflectance theory such as Suits' indicates that observations under overcast conditions are meaningful.

Caution: Lower signals are subject to greater influence by the same noise than full sun readings would be.

5. The reflectance standard must be level, not obscured from the sky by

plants or other surrounding objects - such as the observer - and the radiometer should be perpendicular to it. The same holds for plant canopy observations.

B. Plant observations

1. Table 5 gives the simple correlation between various spectral intervals and percent ground cover, leaf area index, fresh biomass, dry biomass, and plant water content of spring wheat (Aldrich et al. 1978). In the visible (0.40 to 0.74  $\mu\text{m}$ ) and water absorption bands (1.3 to 2.5  $\mu\text{m}$ ) the correlations are negative because plants are obscuring the more reflective soil background. In these wavelengths, plant leaves are efficient absorbers - by pigments and water, respectively. Within the reflective infrared (0.74 to 1.3  $\mu\text{m}$ ) wavelength interval, the correlations are positive due to multiple transmission and reflectance of impinging light by the translucent leaves and leaf layers.
2. Plant height should also be measured routinely. It is an easy, non-destructive measurement that can be taken at sites of repetitive spectral measurements. It will differ somewhat from year to year for a given species at a location just as yields and the other plant parameters do.

Table 5.--The linear correlations (r) of the proposed thematic mapper and LANDSAT MSS wavelength bands with percent soil cover, leaf area index, fresh and dry biomass, and plant water content of spring wheat (from Aldrich et al. 1978)

Wavelength band ( $\mu\text{m}$ )	Percent soil cover	Leaf area index	Fresh biomass	Dry biomass	Plant water content
<b>Thematic Mapper:</b>					
0.45-0.52	-0.79	-0.75	-0.69	-0.54	-0.74
0.52-0.60	- .78	- .74	- .74	- .59	- .78
0.63-0.69	- .84	- .83	- .67	- .48	- .75
0.76-0.90	.91	.89	.68	.48	.76
1.55-1.75	- .81	- .76	- .76	- .61	- .80
2.08-2.35	- .89	- .81	- .81	- .66	- .85
<b>LANDSAT MSS:</b>					
0.5-0.6	- .79	- .75	- .74	- .59	- .78
0.6-0.7	- .84	- .82	- .68	- .49	- .76
0.7-0.8	.79	.80	.47	.27	.55
0.8-1.1	.90	.87	.70	.52	.77

It can be measured by sighting across the tops of plants to a meter stick, as distance ground to tip of uplifted leaf (or inflorescence), or as distance from ground (or crown) to the uppermost leaf ligule (or collar) that completely surrounds the stem or pseudostem. Unfortunately, there seems to be no standardization.

3. Plant population per unit ground area is useful. It need be obtained only once - when the stand is firmly established.

Caution: If sorghum or corn, e.g., are planted in a "clumsy" pattern, some plants will be puny and barren. Thus even in nontillering crops, number of plants present is not necessarily synonymous with the number of heads or ears produced per unit ground area.

4. Episodic events, such as leaf or stem rust infestation, foliage-damaging freezes, insect infestations sufficient to damage the plants or lower yield, hot winds, etc., need to be noted.
5. Phenologic events during plant development, such as those in the Feekes scale for small grains, should be recorded.

#### C. Weather data

Measure and record the following when feasible:

1. Maximum and minimum daily temperature.
2. Insolation.
3. Daily precipitation.

#### D. Sampling

1. All observations should be representative of the field or plot being observed.
  - a. Ideally spectral observations should encompass the area occupied by at least three rows and middles. Not so difficult for small grains, but more of a problem for corn, soybeans, cotton, etc. Alternative here may be a permanently positioned pipe that the pole supporting the radiometer can be inserted into. Then, length of the arm supporting the radiometer becomes a design consideration also. If a permanently positioned pipe is used, and the arm supporting the radiometer is the row width, beginning measurements over the row the permanent pipe is in and continuing every 45° around the circle formed by pivoting the arm yields four observations over rows and four over middles between rows. Those two sets will differ until the leaves overlap in the middles. These readings made looking into the sun could differ from those looking with the sun if proportion of sunlit leaves versus shadow differ in the two look directions.
  - b. Phenological measurements on four or five representative plants that can be averaged have been adequate in my experience. Heading, anthesis, etc., however, are often based on their observation on half the plants or tillers present, so that subjective judgement is almost always involved.

- c. There are statistical guides such as the following for determining number of observations or samples to take: The number of samples required to estimate the true plot mean within 10 percent is given by

$$n = \frac{t^2 S^2}{d^2}$$

wherein,

t is the abscissa of the normal curve which cuts off an area  $\alpha$  at the tails (in this case  $\alpha = 0.05$ ,  $t^2 \sim 4$ ),  $S^2$  is the variance, d is the amount of error allowed, (0.10) (mean).

- d. Experiments should be restricted to what can be done well. A lot of poorly documented treatments are less valuable than a restricted number that are more adequately characterized. (Small is beautiful.)

E. Ground photography

See PHOTOGRAPHIC DETERMINATION OF CANOPY COVER.

F. Terminology

See p. 58-63, Vol. I, "Manual of Remote Sensing," American Society of Photogrammetry, Falls Church, Va. 1975.

## SELECTED REFERENCES

(Literature cited in text is indicated by \*)

- Aase, J. K., and Siddoway, F. H. 1980. Determining winter wheat stand densities using spectral reflectance measurements. *Agron. J.* 72:149-152.
- Aldrich, J. S., Bauer, N. E., Hixson, M. M., and others. 1978. Proc. Int'l Sympos. on Remote Sensing Observation and Inventory of Earth Resources and Endangered Environment 1:629-649.
- \*Allen, W. A., and Richardson, A. J. 1968. Interaction of light with a plant canopy. *Optical Soc. Am.* 58:1023-1031.
- Allen, W. A., Gausman, H. W., Richardson, A. J., and Wiegand, C. L. 1970. Mean effective optical constants of thirteen kinds of plant leaves. *Applied Optics* 9:2573-2577.
- Conaway, J., and van Bavel, C. H. N. 1967. Evaporation from a wet soil surface calculated from a radiometrically determined surface temperature. *J. Applied Meteorol.* 6:650-655.
- \*Deering, D. W., Rouse, J. W., Jr., Haas, R. H., and Schell, H. H. 1975. Measuring "forage production" of grazing units from Landsat MSS data. Proc. Tenth Int. Symp. on Remote Sensing of Environment. Univ. of Michigan, Ann Arbor. P. 1169-1198.

- \*Deering, D. W. 1978. Rangeland reflectance characteristics measured by aircraft and spacecraft sensors. Ph.D. Diss. Texas A&M Univ. College Station, 338 p.
- \*Duggin, M. J. 1977. Likely effects of solar elevation on the quantification of changes in vegetation with maturity using sequential Landsat imagery. *Applied Optics* 16:521-523.
- Ehrler, W. L., Idso, S. B., Jackson, R. D., and Reginato, R. J. 1978. Diurnal changes in plant water potential and canopy temperature of wheat as affected by drought. *Agron. Jour.* 70:999-1004.
- Gausman, H. W., and Allen, W. A. 1973. Optical parameters of leaves of thirty plant species. *Plant Physiol.* 52:57-62.
- Gausman, H. W., Learner, R. W., Noriega, J. R., and Rodriguez, R. R. 1977. Field-measured spectroradiometer reflectances of disked and nondisked soil with and without wheat straw. *Soil Sci. Soc. Amer. J.* 41:793-796.
- Hatfield, J. L. 1979. Canopy temperatures: The usefulness and reliability of remote measurements. *Agron. J.* 71:889-892.
- Hatfield, J. L., Reginato, R. J., Idso, S. B., and Jackson, R. D. 1978. Surface temperature and albedo observations as tools for evapotranspiration and crop-yield estimations. *In COSPAR: The Contribution of Space Observations to Global Food Information Systems*, Edited by E. A. Godby and J. Otterman, Pergamon Press, Oxford and New York. P. 101-104.
- Hatfield, J. L., Reginato, R. J., Jackson, R. D., and others. 1979. Remote sensing of surface temperature and soil moisture, evapotranspiration and yield estimations. *Proc. of 5th Canadian Remote Sens. Symp.*, Victoria, Brit. Col. P. 460-466.
- Holben, B. N., Tucker, C. J., and Fan, C. J. 1980. Spectral assessment of soybean leaf area and leaf biomass. *Photogrammetric Engineering and Remote Sensing* 46:651-656.
- Idso, S. B., Jackson, R. D., and Reginato, R. J. 1976. Compensating for environmental variability in the thermal inertia approach to remote sensing of soil moisture. *Jour. of Appl. Meteorol.* 15:811-817.
- Idso, S. B., Jackson, R. D., and Reginato, R. J. 1976. Determining emittances for use in infrared thermometry: A simple technique for expanding the utility of existing methods. *Jour. of Appl. Meteorol.* 15:16-20.
- Idso, S. B., Jackson, R. D., and Reginato, R. J. 1978. Remote sensing for agriculture water management and crop yield prediction. *Agric. Water Mgmt.* 1:299-310.
- Idso, S. B., Reginato, R. J., Hatfield, J. L. and others. 1980. A generalization of the stress-degree day concept of yield prediction to accommodate a diversity of crops. *Agricultural Meteorol.* 21:205-211.

- Idso, S. B., Schmugge, T. J., Jackson, R. D., and Reginato, R. J. 1975. The utility of surface temperature measurements for the remote sensing of soil water status. *Jour. Geophys. Res. (O&A)* 80:3044-3049.
- Jackson, R. D., Idso, S. B., Reginato, R. J., and Ehrlert, W. L. 1977. Crop temperature reveals stress. *Crops and Soils* 29:10-13.
- \*Jackson, R. D., Pinter, P. J., Jr., Idso, S. B., and Reginato, R. J. 1979. Wheat spectral reflectance: Interaction between crop configuration, sun elevation, and azimuth angle. *Applied Optics* 18:3730-3722.
- Jackson, R. D., Reginato, R. J., and Idso, S. B. 1977. Wheat canopy temperature: A practical tool for evaluating water requirements. *Water Resources Res.* 13:651-656.
- \*Jackson, R. D., Reginato, R. J., Pinter, P. J., Jr., and Idso, S. B. 1979. Plant canopy information extraction from composite scene reflectance of row crops. *Applied Optics* 18:3775-3782.
- Kanemasu, E. T. 1974. Seasonal canopy reflectance patterns of wheat, sorghum, and soybean. *Remote Sensing of Environment* 3:43-47.
- \*Kauth, R. J., and Thomas, C. S. 1976. The tasseled cap - A graphic description of the spectral-temporal development of agricultural crops as seen by Landsat. *Proc. Symp. on Machine Processing of Remotely Sensed Data.* P. 41-51. West Lafayette, Ind.
- Kimes, D. S., Idso, S. B., Pinter, P. J., Jr., and others. 1980. Complexities of nadir-looking radiometric temperature measurements of plant canopies. *Applied Optics* 19:2162-2168.
- Kimes, D. S., Idso, S. B., Pinter, P. J., Jr., and others. View angle effects in radiometric measurement of plant canopy temperatures. *Remote Sensing of Environment.* (In press).
- Kimes, D. S., Markham, B. L., Tucker, C. J., and McMurtrey, J. E. 1980. Temporal relationships between spectral response and agronomic variables of a corn canopy. NASA/GSFC TM. (In preparation).
- \*Larsen, H. D. 1958. Compiler, Rinehart Mathematical Tables, Formulas and Curves, Rinehart and Co., New York. P. 192-193.
- Learner, R. W., and LaRocca, A. J. 1973. Calibration of field spectroradiometers. *Optical Engineering* 12:124-130.
- \*Learner, R. W., Noriega, J. R., and Wiegand, C. L. 1978. Seasonal changes in reflectance of two wheat cultivars. *Agron. J.* 70:113-118.
- LeMaster, E. W., Chance, J. E., and Wiegand, C. L. 1980. A seasonal verification of the Suit's spectral reflectance model for wheat. *Photogrammetric Engineering and Remote Sensing* 46:107-114.

- Millard, J. P., Hatfield, J. L., and Goettelman, R. C. 1979. Equivalence of airborne and ground-acquired wheat canopy temperatures. *Remote Sensing of Environment* 8:273-275.
- Millard, J. P., Jackson, R. D., Goettelman, R. C., and others. 1978. Crop water stress assessment using an airborne thermal scanner. *Photogrammetric Engineering and Remote Sensing* 44:77-85.
- Millard, J. P., Jackson, R. D., Goettelman, R. C., and others. 1977. Airborne monitoring of crop canopy temperatures for irrigation scheduling and yield prediction. *Proc. 11th Intl. Symp. on Remote Sensing of the Environment*. P. 1453-1461. Ann Arbor, Mich.
- Millard, J. P., Reginato, R. J., Idso, S. B., and others. 1980. Experimental relations between airborne and ground measured wheat canopy temperatures. *Photogrammetric Engineering and Remote Sensing* 46:221-224.
- \*Pearson, R. L., Miller, L. D., and Tucker, C. J. 1976. A hand-held spectral radiometer to estimate gramineous biomass. *Applied Optics* 16:416-418.
- Pinter, P. J., Jr., Stanghellini, M. E., Reginato, R. J., and others. 1979. Remote detection of biological stresses in plants with infrared thermometry. *Science* 205:585-588.
- Reginato, R. J., Idso, S. B., Vedder, J. F., and others. 1976. Soil water content and evaporation determined by thermal parameters obtained from ground-based and remote measurements. *Jour. Geophys. Res. (Oceans and Atmospheres)* 81:1617-1620.
- Richardson, A. J., Escobar, D. E., Gausman, H. W., and Everitt, J. H. 1980. Comparison of LANDSAT-2 and field spectrometer reflectance signatures of south Texas rangeland plant communities. *Sixth Symp. Machine Processing of Remotely Sensed Data*, Purdue Univ. (In press).
- \*Richardson, A. J., Wiegand, C. L., Gausman, H. W., and others. 1975. Plant, soil, and shadow reflectance components of row crops. *Photogrammetric Engineering and Remote Sensing* 41:1401-1407.
- \*Richardson, A. J., and Wiegand, C. L. 1977. Distinguishing vegetation from soil background information. *Photogrammetric Engineering and Remote Sensing* 43:1541-1552.
- \*Rider, P. R. 1947. *Analytic Geometry*. The MacMillan Co., New York. P. 63.
- \*Robinson, B. F., and Biehl, L. L. 1979. Calibration procedures for measurement of reflectance factor in remote sensing field research. *Society of Photo-optical Instrumentation Engineers, Vol. 196, Measurements of Optical Radiations*. P. 16-26.
- \*Rouse, J. W., Jr., Haas, R. H., Schell, J. A., and Deering, D. W. 1973. Monitoring the vernal advancement and retrogradation (green wave effect) of natural vegetation. *Prog. Rep. RSC 1978-1, Remote Sensing Center, Texas A&M Univ., College Station*. 93 p. (NTIS No. E73-10693).

- \*Silva, L. F. 1978. Radiation and instrumentation in remote sensing. *In* P. H. Swain and S. M. Davis, eds., *Remote Sensing - The Quantitative Approach*. McGraw-Hill, Inc., New York. 396 p.
- \*Slater, P. N. 1979. A re-examination of the Landsat MSS. *Photogrammetric Engineering and Remote Sensing* 45:1479-1485.
- Stone, L. R., Kanemasu, E. T., and Horton, M. L. 1975. Grain sorghum canopy temperature as influenced by clouds. *Remote Sensing of Environment* 4:177-181.
- \*Suits, C. H. 1975. The nature of electromagnetic radiation. *In* R. G. Reeves (ed.), *Manual of Remote Sensing*, Vol. 1, p. 51-73.
- \*Swain, P. H., and Davis, S. M. 1978. *Remote Sensing - The Quantitative Approach*. McGraw-Hill, Inc., New York. 396 p.
- Thomas, J. R., and Oerther, G. F. 1972. Estimating nitrogen content of sweet pepper leaves by reflectance measurements. *Agron. J.* 64:11-13.
- \*Threlkeld, J. L. 1962. *Thermal Environmental Engineering*. Prentice-Hall, Englewood Cliffs, N.J. P. 313-321.
- \*Tucker, C. J. 1978a. A comparison of satellite sensor bands for vegetation monitoring. *Photogrammetric Engineering and Remote Sensing* 44:1369-1380.
- \*Tucker, C. J. 1978b. Hand-held radiometer studies of agricultural crops in situ: A new and promising approach. *In Proc. of Remote Sensing for Observation and Inventory of Earth Resources and the Endangered Environment*, Freiburg, Germany. P. 667-672.
- \*Tucker, C. J. 1979. Red and photographic infrared linear combinations for monitoring vegetation. *Remote Sensing of Environment* 8:127-150.
- Tucker, C. J. 1980a. A spectral method for determining the percentage of green material in a cut herbage sample. *Remote Sensing of Environment* 9:175-181.
- Tucker, C. J. 1980b. Remote sensing of leaf water content in the near infrared. *Remote Sensing of Environment*. (In press).
- Tucker, C. J., Elgin, J. H., and McMurtrey, J. E. 1979. Temporal spectral measurements of corn and soybean crops. *Photogrammetric Engineering and Remote Sensing* 45:643-653.
- Tucker, C. J., Elgin, J. H., and McMurtrey, J. E. 1980. Relationship of crop radiance to alfalfa agronomic values. *International J. of Remote Sensing* 1:69-75.
- Tucker, C. J., Elgin, J. H., McMurtrey, J. E., and Fan, C. J. 1979. Monitoring corn and soybean crop development with hand-held radiometer spectral data. *Remote Sensing of Environment* 8:237-248.
- Tucker, C. J., Holben, B. N., Elgin, J. H., and McMurtrey, J. E. 1980. Remote sensing of total dry matter accumulation in winter wheat. NASA/GSFC TM-80631.

Tucker, C. J., Holben, B. N., Elgin, J. H., and McMurtrey, J. E., III. 1980. Relationship of spectral data to grain yield variation. Photogrammetric Engineering and Remote Sensing 46:657-666.

\*Tucker, C. J., Jones, W. H., Kley, W. A., and Sundstrom, C. J. 1980. A three band hand-held radiometer for field use. NASA/GSFC TM-80641.

\*Turner, R. E., Malila, W. A., and Nalepka, R. F. 1971. Importance of atmospheric scattering in remote sensing, or everything you've always wanted to know about atmospheric scattering but were afraid to ask. Proc. of the Seventh Int. Symp. on Remote Sens. of Environ. 111:1651-1697.

\*Turner, R. E., and Spencer, H. H. 1972. Atmospheric model for correction of spacecraft data. Proc. of the Eighth Int. Symp. on Remote Sens. of Environ. 11:895-934.

\*Ungar, S. G., Collins, W., and Coiner, J. 1977. Atlas of selected crop spectra of Imperial Valley, California. NASA/GSFC.

Walker, C. K., and Hatfield, J. L. 1979. Test of the stress-degree-day concept using multiple planting dates of red kidney beans. Agron. J. 71:967-971.

Wiegand, C. L., Gausman, H. W., and Allen, W. A. 1972. Physiological factors and optical parameters as bases of vegetation discrimination and stress analysis. Proc. Seminar on Operational Remote Sensing. American Society of Photogrammetry, Falls Church, Va. P. 82-102.

\*Wiegand, C. L., Gausman, H. W., Cuellar, J. A., and others. 1974. Vegetation density as deduced from ERTS-1 MSS response. Proc. 3rd Earth Resources Technology Satellite-1 Symp., Vol. I, p. 93-115.

\*Wiegand, C. L., Richardson, A. J., and Kanemasu, E. T. 1979. Leaf area index estimates for wheat from LANDSAT and their implications for evapotranspiration and crop modeling. Agron. J. 71:336-342.

\*Williams, T. H. Lee. 1979. An error analysis of the photographic technique for measuring percent vegetation cover. Soil Sci. Soc. Am. J. 43:578-582.

\* U.S. GOVERNMENT PRINTING OFFICE: 1980-789-383/47